PNNL-10748
UC-2030

Thermal and Combined Thermal and Radiolytic Reactions Involving Nitrous Oxide, Hydrogen, Nitrogen, and Ammonia in Contact with Tank 241-SY-101 Simulated Waste

S. A. Bryan
L. R. Pederson

February 1996

Prepared for the U.S. Department of Energy
under Contract DE-AC06-76RLO 1830

Pacific Northwest National Laboratory
Operated for the U.S. Department of Energy
by Battelle

Battelle

PNNL-10748

PACIFIC NORTHWEST NATIONAL LABORATORY
operated by
BATTELLE
for the
UNITED STATES DEPARTMENT OF ENERGY
under Contract DE-AC06-76RLO 1830

Printed in the United States of America

Available to DOE and DOE contractors from the Office of Scientific and Technical Information, P.O. Box 62, Oak Ridge, TN 37831; prices available from (615) 576-8401.

Available to the public from the National Technical Information Service, U.S. Department of Commerce, 5285 Port Royal Rd., Springfield, VA 22161

PNL-10748
UC-2030

Thermal and Combined Thermal and Radiolytic Reactions Involving Nitrous Oxide, Hydrogen, Nitrogen, and Ammonia in Contact with Tank 241-SY-101 Simulated Waste

S. A. Bryan
L. R. Pederson

February 1996

Prepared for
the U.S. Department of Energy
under Contract DE-AC06-76RLO 1830

Pacific Northwest National Laboratory
Richland, Washington 99352

Executive Summary

Work described in this report was conducted at Pacific Northwest National Laboratory (PNNL)[a] for the Flammable Gas Safety Project, the purpose of which is to develop information needed to support Westinghouse Hanford Company (WHC) in their efforts to ensure the safe interim storage of wastes at the Hanford Site. Described in this report are the results of tests to evaluate the rates of thermal and combined thermal and radiolytic reactions involving flammable gases in the presence of Tank 241-SY-101 simulated waste. Flammable gases generated by the radiolysis of water and by the thermal and radiolytic decomposition of organic waste constituents may themselves participate in further reactions. Examples include the decomposition of nitrous oxide to yield nitrogen and oxygen, the reaction of nitrous oxide and hydrogen to produce nitrogen and water, and the reaction of nitrogen and hydrogen to produce ammonia. The composition of the gases trapped in bubbles in the wastes might therefore change continuously as a function of the time that the gas bubbles are retained.

The decomposition of nitrous oxide, reactions between nitrous oxide and hydrogen, reactions between nitrogen and hydrogen, and decomposition reactions of ammonia in contact with Tank 241-SY-101 simulated waste under thermal and combined thermal and radiolytic conditions were investigated in the temperature range of 60 to 150°C. Radiation doses ranged from 0 to more than 10 Mrad (^{60}Co), while reaction times extended to 70 hours. Reactions were performed in stainless steel vessels that allowed continuous monitoring of gas pressures. Gas compositions were evaluated using mass spectrometry and infrared spectrometry.

The primary radiolytic and thermal products of nitrous oxide decomposition were nitrogen, oxygen, and nitrogen dioxide. Under thermal-only conditions, the extent of nitrous oxide decomposition was less than that for the companion experiment under combined thermal and radiolytic conditions. However, the thermal decomposition in the presence of simulated waste was significant compared with that observed in earlier tests in the absence of simulated waste (Bryan and Pederson 1995). G-values measured for the decomposition of nitrous oxide in the presence of simulated waste showed a significant temperature dependence, consistent with a surface reaction with nitrous oxide contributing to the decomposition reaction. $G(N_2O)$ ranged in value from -7 to -17 in the systems containing wet and dried simulated waste.

In contrast, $G(N_2O)$ for the gas phase decomposition of nitrous oxide was determined to be constant at -12 molecules/100 eV, in good agreement with literature values. No temperature dependence of $G(-N_2O)$ was apparent from 60 to 150°C. Nitrogen dioxide yields decreased with increasing temperature, while nitrogen yields increased with increasing temperature. Assuming a gamma dose rate of 1000 R/h in the actual wastes, and assuming that nitrous oxide composes $\approx 30\%$ of the gases trapped in the nonconvecting layer, it is estimated that $\approx 1\%$ of the retained nitrous oxide could be consumed by these gas-phase radiolytic reactions per year. However, the thermal decomposition of nitrous oxide contributes significantly to the total decomposition of nitrous oxide when in contact with simulated waste.

(a) Pacific Northwest National Laboratory is operated by Battelle for the U. S. Department of Energy under Contract DE-AC06-76RLO 1830.

Catalysis of nitrous oxide decomposition by solid phases is a significant possibility. At least some of the gases will be retained as bubbles attached to solid particles, in response to surface tension forces. Thus the gases will be in intimate contact with tank solids, which include sodium aluminate, sodium nitrate, sodium nitrite, sodium carbonate, and other phases. The temperature dependence of the G-value for the decomposition of nitrous oxide in the presence of wet or dried waste simulant solids shows that a thermal component is involved. By contrast, the gas phase reaction showed no thermal sensitivity over the same temperature range. In addition, while the thermal reaction of nitrous oxide in the presence of simulated waste solids showed significant conversion of nitrous oxide to other gas products, under similar conditions the gas phase reaction showed no conversion under thermal conditions alone. Based on data within this report, and assuming a pseudo-zero order, surface catalyzed reaction for the decomposition of nitrous oxide in contact with the waste, it can be estimated that between ≈ 20 to $\approx 90\%$ of the nitrous oxide could be decomposed in one year.

In earlier studies, it was found that under thermal-only conditions the principal products of the gas phase reaction of nitrous oxide with hydrogen were nitrogen, oxygen, water, and a very small concentration of ammonia (Bryan and Pederson 1995). Under combined thermal and radiolytic conditions, while similar products were found as for thermal-only conditions, the extent of nitrous oxide and hydrogen consumption and of ammonia formation was considerably greater.

Similar trends were observed for the reaction of nitrous oxide with hydrogen in contact with simulated waste and for the reaction of these gases in the gas phase alone. The primary product of the reaction of nitrous oxide with hydrogen in contact with wet or dried simulated waste is nitrogen, followed by oxygen and other oxides of nitrogen. Much more nitrogen and oxygen were produced with irradiation than with thermal conditions alone. The decomposition of hydrogen and nitrous oxide was temperature-dependent, especially in the irradiated sample in contact with wet simulated waste. Nitrogen production increases with increasing temperature following the consumption of nitrous oxide for these reactions.

The mass balance for gas-phase nitrogen was not good in the reactions of nitrous oxide with hydrogen in contact with wet or dried simulated waste. The gain of nitrogen is more than can be accounted for by the loss of nitrous oxide alone. The reason for the apparent discrepancy is most likely due to the production of nitrogen from the solid phase sources of nitrogen, nitrite, and nitrate. These solid phase reactants have been shown in earlier tests to produce nitrogen under similar temperature and irradiation conditions in simulated wastes (Bryan and Pederson 1994; Bryan et al. 1992a). In contrast to the work reported for the gas phase reactions of nitrous oxide and hydrogen (Bryan and Pederson 1995), when these gases are in contact with simulated waste no measurable amount of ammonia is produced.

Ammonia was the principal product of the thermal and combined thermal and radiolytic reactions of nitrogen and hydrogen. Radiolytic ammonia yields showed a strong inverse relation with radiation dose. For low radiation doses, $G(NH_3)$ was nearly 1 molecule/100 eV, in good agreement with literature values. However, this yield decreased to approximately 0.01 molecules/100 eV for doses greater than 10 Mrad. From the literature, the value of $G(-NH_3)$ is known to be as much as a factor of ten greater than $G(NH_3)$ depending on temperature and gas partial pressures. As the concentration of NH_3 increased in the gas mixture, so did the relative importance of ammonia decomposition to nitrogen.

The lack of significant quantities of ammonia in either the wet or dried SY1-SIM-92A systems is counter to the observation of this product when only gas-phase nitrogen and hydrogen were present. There is little doubt that this product should form under nearly identical conditions, with the exception of added SY1-SIM-92A simulated waste being present. The absence of ammonia in the systems with waste present is most likely attributed to the reaction of the oxidants nitrite and nitrate with ammonia forming nitrogen, nitrous oxide, and other oxides of nitrogen, which effectively removes ammonia as it is being formed.

The decomposition of ammonia was apparent for the reaction systems containing wet and dry SY1-SIM-92 waste simulant, in both thermal-only and thermal and radiolytic conditions, over the temperature range 60 to 150°C. The reaction of ammonia under thermal-only conditions and under radiolytic and thermal conditions shows a definite trend with increasing temperature. Although there is a definite temperature dependence to the decomposition, the decomposition is more prominently facilitated in the radiolytic experiments. Nitrogen and hydrogen are the principal products of the radiolytic decomposition of ammonia in contact with the wet or dried simulated waste. Hydrogen is produced in a greater fraction in the wet system than in the dried simulated waste system, most likely due to its co-production by radiolysis of water. Radiolysis of ammonia in the gas phase, coupled with thermal decomposition, may be an important means by which the ultimate concentration of ammonia is limited in Hanford Site wastes.

Contents

Figures

Tables

1.0 Introduction

This report summarizes progress in evaluating the rates of chemical reactions involving nitrogen, nitrous oxide, hydrogen, and ammonia in the gas phase under both thermal and combined thermal and radiolytic conditions. Reactions between gases that are trapped in bubbles in Hanford tank wastes may lead to altered gas product distributions, depending on the length of time that the gas bubbles have remained trapped. Work described in this report was conducted at Pacific Northwest National Laboratory under the Flammable Gas Safety Project, whose purpose is to develop information needed to support the interim safe storage of nuclear and chemical wastes at the Hanford Site.

Among the gaseous products of thermal and radiolytic reactions that occur in the wastes stored in Hanford double-shell tanks are hydrogen, nitrous oxide, nitrogen, ammonia, and methane (Babad et al. 1991, 1992; Ashby et al. 1992; LANL 1994). From studies using simulated wastes, the kinetics of formation and the stoichiometry of these gaseous products have been shown to be sensitive to the composition of the waste mixture (Delegard 1980; Jansky and Meissner, in Reynolds et al. 1991; Ashby et al. 1992, 1993, 1994a,1994b; Meisel et al. 1991, 1992, 1993; Bryan et al. 1992, 1993; Bryan and Pederson 1994). Nitrite, hydroxide, aluminate, transition metal and chloride ion concentrations, the identity and concentration of organic waste components, temperature, and radiation dose/dose rate all affect gas generation behavior.

Some of the gaseous products of water radiolysis and waste decomposition reactions are known to become trapped as gas bubbles within the nonconvecting layer of Hanford tank wastes, a layer that contains a high fraction of solids (Herting et al. 1992a, 1992b; Reynolds 1992). Before the mixer pump was installed in Tank 241-SY-101, gases were retained and periodically released in gas release events (GREs) (Babad et al. 1992; U. S. Department of Energy 1994). On occasion those GREs led to hydrogen concentrations slightly in excess of the lower flammability limit. Gases may also be dissolved in the liquid portion of the waste. Except for ammonia, gases formed from waste decomposition and water radiolysis are sparingly soluble in the highly concentrated, caustic waste mixtures (Norton and Pederson 1994, 1995; Pasamehmetoglu et al. 1994)

For bubbles to be retained in the nonconvecting, sludge layer of Hanford wastes, the sludge must resist the buoyant force that would otherwise cause the gas bubble to rise. Bubble retention has been classified into five mechanisms (Gauglitz et al. 1994a, 1994b): 1) yield strength or viscous retention; 2) as armored bubbles, where gas bubbles become surrounded by attached solid particles; 3) as a gas bubble attached to a single solid particle; 4) as solid particle, gas bubble aggregates; and 5) as dendritic bubbles that fill spaces between solid particles. The morphology of bubbles retained in the sludge has been related to the Bond number (Gauglitz et al. 1994a, 1994b), which is determined by the differences in densities between the sludge and liquid, the depth into the sludge layer that the bubbles are trapped, the gas/liquid interfacial tension, and the pore throat diameter between sludge particles. Gases trapped deep within the sludge layer are most likely to be collected in dendritic bubbles, while those closer to the surface will tend to be more spherical in shape and will displace solid particles. A schematic diagram of bubble morphologies deep in the sludge and near the surface of the waste is given in Fig ure 1.1, adapted from Gauglitz et al. (1994b).

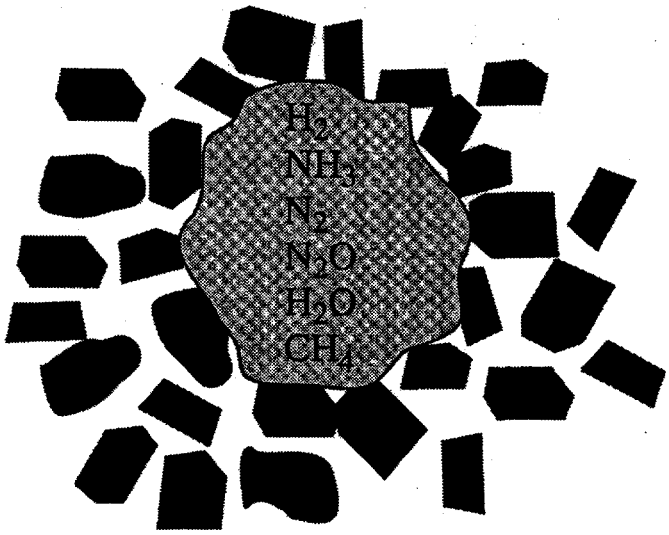

Gas Bubble That Displaces
Solid Particles

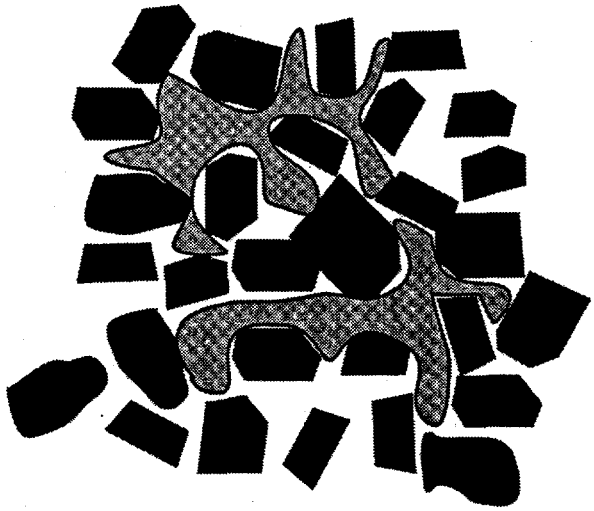

Dendritic Bubbles That Displace
Liquid from Between Particles

Figure 1.1. Gas Bubbles Containing Hydrogen, Ammonia, Nitrogen, Nitrous Oxide, Water, and Methane Surrounded by Solid Particles

Further thermal and radiolytic reactions may also occur involving gases trapped in the Hanford wastes. Ashby et al. (1994b) have shown that nitrous oxide decomposes to nitrogen and oxygen in tests with simulated waste mixtures at 90 to 120°C. They attributed nitrous oxide decomposition reactions to catalysis by the glass walls of their reaction vessels. Bryan and Pederson (in Strachan and Schulz 1993) also found that nitrous oxide decomposed in tests with simulated wastes conducted in stainless steel vessels, particularly under radiolytic conditions. More recently, Bryan and Pederson (1994) described reactions of nitrogen and hydrogen to yield ammonia and of nitrous oxide and hydrogen reactions to yield ammonia, nitrogen, oxygen, and nitrogen dioxide. Since gas products of radiolytic and thermal reactions in simulated wastes participate in further reactions, observed gas distributions in actual wastes may well vary as a function of the time the gases have remained trapped.

In this study we evaluated thermal and combined thermal and radiolytic reactions that involve gases known to be produced in the wastes stored in Tank 241-SY-101 and expected to be present in similar wastes in other tanks. Unlike measurements reported previously (Bryan and Pederson 1994), gas reactions in this study were conducted in the presence of dried or wet simulated waste solids. These solids may serve as catalysts, thereby enhancing the rates of reactions and/or changing product distributions. Specific reactions considered in this study were 1) nitrous oxide decomposition; 2) nitrogen and hydrogen reactions, where ammonia is the primary product; 3) nitrous oxide and hydrogen reactions, where ammonia, nitrogen, and nitrogen dioxide are the primary products; and 4) ammonia decomposition, where nitrogen and hydrogen are the primary products. The gas-generating capacity of wet and dried simulated waste solids were also assessed. Reactions were studied in the temperature range of 60 to 150°C with and without gamma radiation present.

2.0 Experimental Methods for Gas Measurements and Sample Irradiation

Sample irradiation experiments were performed in the Gamma Irradiation Facility operated by PNNL and located in the 3730 Building in the 300 Area. The facility contains 37 stainless steel irradiation tubes positioned in a 2.1-m (7-ft)-diameter by 4.2-m (13-ft-8-in.)-deep stainless steel tank. Two arrays of ^{60}Co with a combined inventory of 32 kCi are located near the bottom of the tank. For radiation shielding purposes, the tank is completely filled with water; a concrete wall, 1.1 m (3.5 ft) in height, surrounds the top of the tank. The irradiation tubes, which are sealed on the bottom, vary in length from 4.9–5.5 m (16 to 18 ft) and in diameter from 4.6 to 15 cm (1.8 to 6 in.). The irradiation dose rate of the tubes ranges from 2×10^6 R/h to 2×10^2 R/h. The uniform flux region varies from ~15 cm (6 in.) for the tubes closest to the sources to greater than 30 cm (12 in.) for the tubes farthest from the sources. All flux measurements of the tubes are traceable to the National Bureau of Standards.

The ^{60}Co gamma irradiation facility was calibrated using an ion chamber and thermoluminescent dosimeters (TLDs). The ion chamber measurements were made using a Capintec® PR-06C chamber with built-up cap, S/N CIIG 64053, and a Keithly electrometer, S/N 115092. The ion chamber is a transfer standard that carries a calibration certificate for ^{60}Co from the National Bureau of Standards. Its calibration was confirmed by direct comparison with a Capintec® PM-30 chamber, which also carries a calibration certificate for ^{60}Co from the National Bureau of Standards. Calibration measurements were performed in Gamma Access Tube 21 with a chamber centered 15, 20, and 25 cm (6, 8, and 10 in.) from the bottom of the tube. Calibration results are kept on file in the gamma facility.

The TLDs were calibrated by placing TLD packets in the lucite rod at positions corresponding to the National Bureau of Standards traceable ion chamber calibrations. A series of TLD exposures for varying times provided data to determine the TLD response versus exposure time. The results of the TLD measurements were used to calculate the dose rate (R/h) in all the ^{60}Co exposure tubes in the gamma facility. Current dose rates are adjusted for natural decay of the ^{60}Co source. Sources of error for gamma tube calibration include exposure geometry, ion chamber measurement, TLD response, calibration fit, and source decay errors. The overall average tube calibration uncertainty is estimated to be 6%.

Materials, capsules, and test systems were lowered into the irradiation tubes to the desired flux manually or with a half-ton crane. They were left in the tubes for a specific amount of time to attain the required exposure. There is no activation associated with the gamma irradiation, so the materials can be transported to other facilities for examination after removal from the tubes.

The stainless steel reaction vessels used in this study were wrapped with heat tape. Temperatures were regulated by temperature controllers monitored by recording thermocouples. The pressures of the reaction vessels were measured using pressure transducers connected to the gas manifold line of each vessel. Small-diameter stainless steel tubing (0.06 cm [0.023 in.] inner diameter) connected the reaction vessel to the gas manifold system.

Total moles of gases produced were calculated based on the measured pressure, temperature, and known volume of the gas phase of the reaction vessel. The volumes of the reaction vessels were

determined gravimetrically by filling them with water. The volumes of the pressure sensor, valves, and miscellaneous fittings were determined from pressure/volume relationships using a calibrated gas manifold system.

In virtually all cases, only one sample was run to obtain each point. Each radiolytic yield or G-value reported was a separate, independent experiment, not the same sample analyzed at different times. We assume that the gases were well-mixed, a reasonable assumption. Samples were withdrawn through the capillary line into an evacuated bulb. The volume of the capillary line was small—less than 2 mL—whereas the reaction vessel volume was ≈ 1 liter in most cases and ≈ 50 mL for the high dose rate experiments, and the collection bulb volume was ≈ 30 mL. Because gases move by viscous flow through the capillary tube in this pressure regime, we do not anticipate that significant errors are introduced by using this procedure.

Analyses were performed to determine the mole percent of the components within the gas phase of each reaction vessel using the Mass Spectroscopy Facility operated by PNNL and located in the 325 Building. The amounts of specific gases generated were calculated from the total moles of gas generated and the mole percent data. Recovery of ammonia, which was assessed by filling the experimental apparatus with a known concentration of ammonia followed by sample extraction and analysis by mass spectroscopy, was within 10% of expected results using a commercial ammonia gas standard.

G-values are calculated by dividing the number of molecules of product formed (or reactant consumed) in the radiolytic reaction by the total energy absorbed by all of the components present in the reaction vessel. A companion control, thermal-only experiment was performed for each radiolytic experiment to assess the contribution of the thermal component on gas generation. Inert gases affect the rates of radiolytically driven reactions, so when we calculate G-values for a particular reaction, energy absorbed by inert gases such as argon is included. This energy is transferred to reacting molecules by collisions (O'Donnell and Sangster 1970). Changes in reaction composition are recorded as changes in moles of gaseous reactant per kilogram total mass per day (mol/kg/day).

Hanford Tank 241-SY-101 simulated waste SY1-SIM-92A, prepared using standard procedures (Bryan and Pederson 1994), was used in each experiment containing solids. This simulant contains major and minor inorganic components known to be present in actual wastes. Organic components were omitted from the simulant to avoid complications associated with gas generation reactions. The solid phase was separated from the bulk simulant by centrifugation. Simulated waste was introduced into each experiment as wet or dried centrifuged solids. The dried solids were prepared by heating the wet centrifuged solids to 160°C for several weeks, then grinding the simulant in a ball mill. One batch of wet and dried simulated waste was prepared for the entire set of experiments. The water content of the wet and dried simulants was measured by thermal gravimetric analysis to be 31.9% and $<1.0\%$, respectively.

The reaction containers used in this study were stainless steel Parr® reaction vessels, approximately 1 L in volume. The vessels were dried at approximately 110°C before filling. After adding the solid simulated waste material, reaction systems (for thermal and thermal/radiolytic reactions) were flushed with inert gas by evacuating and purging argon gas through the vessels, attached by stainless steel tubing to a gas manifold system, at least three times. Reaction systems were then filled with the reaction gas mixture by equilibrating the reaction gas into the evacuated vessels from the gas manifold

system simultaneously. The gas pressure in each reaction system was atmospheric at the time the vessel was closed, immediately before the start of the experiment. The sampling methodology and the gas manifold system used to connect multiple reaction vessels were described in detail in Bryan and Pederson (1994).

The container walls may have some effect on radiolysis results. We did not conduct tests in different types of vessels to directly evaluate such effects. However, it is noted that reasonably good agreement between G-values reported in the literature and those determined here were obtained for low dose rates for several reactions of interest. The principal purpose of this study was to assess the effects of simulated waste solids on reactions involving gases, which is accomplished by comparing the present results with those of a previous study (Bryan and Pederson 1994). Even if wall effects did contribute in some small way, we expect such effects to be similar whether simulated waste solids were or were not present.

There are several contributors to gas measurement error; uncertainties in temperature are believed to be the most important. For an activation energy of 25 kcal/mole, approximately that reported for gas generation and related reactions (Delegard 1980; Ashby et al. 1993; Meisel et al. 1993; Orth et al. 1993; Schmidt et al. 1993, 1994), a one-degree difference in temperature from 90°C would yield a 10% change in rate, a two-degree difference would yield a 20% change in rate, and a five-degree difference would yield a 60% change. The 1-L reaction vessels were independently temperature-controlled and monitored throughout the tests to within ± 0.5°C, leading to a 5% error because of changes in thermal reaction rates and assuming a 25 kcal/mole activation energy. Other direct contributors to measurement uncertainties are mass spectroscopy analyses and pressure measurements. The precision in mass spectroscopy measurements was approximately 2%; the precision in pressure measurements is approximately 1%. The absolute reaction vessel volume was known to better than 1%, while the quantity of reactants introduced into the reaction vessel was known to better than 0.1% for solid and liquid samples and 1% for gaseous reactants. Analyses of gas generation from repeated experiments provided estimates of errors for determining gas product formation in gas phase reactions and in gas generation from simulated wastes. The relative error for replicate gas samples using the reaction vessels ($\approx$ 1-L capacity) is approximately 5%. The calculated root-mean-square error from all of the contributors to measurement uncertainty is dominated by the estimated temperature contribution and dose rate calibration uncertainty, or 8%. Uncertainties in gas analysis data were also discussed in detail in Bryan and Pederson (1994).

The simulant SY1-SIM-92A was chosen as a waste simulant for this study because it represents the first attempt to match, as closely as possible, the inorganic components and concentrations present in the actual waste in Tank 241-SY-101 (Strachan 1993). Based on Window C core sampling and analysis (Herting 1992), the simulant contains all the major inorganic components plus many of the minor constituents at chemically significant levels. The waste simulant composition is given in Table 2.1.

The test matrix used for this study is given in Table 2.2, which shows the number of experiments performed with each cover gas, each temperature, whether the waste simulant waste wet or dried, and the gamma dose rate used for each experiment. As this table indicates, there were 80 independent experiments performed during the course of this work.

Table 2.1. Concentrations of Components Used in SY1-SIM-92A Simulated Waste

Component	M (mole/L)	Weight%
organic	0.00	0.00
NaCl	0.526	2.08
Na_3PO_4 * 12 H_2O	0.179	4.60
$NaNO_2$	3.95	18.42
$NaNO_3$	2.2	12.63
Na_2CO_3	0.4	2.86
NaF	0.1	0.28
Na_2SO_4	0.032	0.31
$CaCl_2$	0.0083	0.06
KCl	0.146	0.74
$Cr(NO_3)_3$ * 9 H_2O	0.1051	2.84
$Cu(NO_3)_2$ * 2.5 H_2O	0.00021	0.00
$Fe(NO_3)_3$ *9 H_2O	0.0074	0.20
$Ni(NO_3)_2$ * 6 H_2O	0.0021	0.04
NaOH	2.45	6.62
$NaAlO_2$ * 0.21NaOH *0.14H_2O	2.05	12.84
H_2O	—	35.47
TOTAL		100

Experiments 1–16 were performed under an inert gas (argon) to determine the reactivity and gas generation capacity of the waste without an added reactive cover gases. Experiments 17–32 were conducted with nitrous oxide cover gas to determine the reactivity of this gas with the wet and dried waste simulant. Experiments 33–48 were carried out under a cover gas containing 2% nitrous oxide and 2% hydrogen (balance argon) in the presence of the wet and dried simulated waste to determine the reactivity of these gases in the presence of the simulated waste. Experiments 49–64 were performed with a cover gas of 95% nitrogen and 5% hydrogen to determine the reactivity of these gases with simulated waste. Experiments 65–80 were executed using 10% ammonia (balance argon) as the reactive cover gas. This series of experiments was conducted to determine the rate of decomposition of ammonia with the aid of solids from simulated waste.

The experimental results from the reactions of these five cover gases with the simulated waste are described in detail in Sections 3.1 through 3.5 of this report.

Table 2.2. Reaction Matrix Used for Gas Generation Experiments

Reaction Matrix				
Sample #	**Cover Gas**	**Wet/Dry**	**Temperature, °C**	**Dose rate, R/h**
1	Argon	dry	60	0
2	Argon	dry	60	1.65E+06
3	Argon	dry	90	0
4	Argon	dry	90	1.65E+06
5	Argon	dry	120	0
6	Argon	dry	120	1.65E+06
7	Argon	dry	150	0
8	Argon	dry	150	1.65E+06
9	Argon	wet	60	0
10	Argon	wet	60	1.65E+06
11	Argon	wet	90	0
12	Argon	wet	90	1.65E+06
13	Argon	wet	120	0
14	Argon	wet	120	1.65E+06
15	Argon	wet	150	0
16	Argon	wet	150	1.65E+06
17	100% N_2O	dry	60	0
18	100% N_2O	dry	60	8.70E+04
19	100% N_2O	dry	90	0
20	100% N_2O	dry	90	8.70E+04
21	100% N_2O	dry	120	0
22	100% N_2O	dry	120	8.70E+04
23	100% N_2O	dry	150	0
24	100% N_2O	dry	150	8.70E+04
25	100% N_2O	wet	60	0
26	100% N_2O	wet	60	8.70E+04
27	100% N_2O	wet	90	0
28	100% N_2O	wet	90	8.70E+04
29	100% N_2O	wet	120	0
30	100% N_2O	wet	120	8.70E+04
31	100% N_2O	wet	150	0
32	100% N_2O	wet	150	8.70E+04
33	2% N_2O, 2% H_2 in Ar	dry	60	0
34	2% N_2O, 2% H_2 in Ar	dry	60	1.50E+04
35	2% N_2O, 2% H_2 in Ar	dry	90	0
36	2% N_2O, 2% H_2 in Ar	dry	90	1.50E+04
37	2% N_2O, 2% H_2 in Ar	dry	120	0
38	2% N_2O, 2% H_2 in Ar	dry	120	1.50E+04
39	2% N_2O, 2% H_2 in Ar	dry	150	0
40	2% N_2O, 2% H_2 in Ar	dry	150	1.50E+04

Table 2.2. (contd)

Reaction Matrix				
Sample #	**Cover gas**	**Wet/Dry**	**Temperature, °C**	**Dose rate, R/h**
41	2% N_2O, 2% H_2 in Ar	wet	60	0
42	2% N_2O, 2% H_2 in Ar	wet	60	1.50E+04
43	2% N_2O, 2% H_2 in Ar	wet	90	0
44	2% N_2O, 2% H_2 in Ar	wet	90	1.50E+04
45	2% N_2O, 2% H_2 in Ar	wet	120	0
46	2% N_2O, 2% H_2 in Ar	wet	120	1.50E+04
47	2% N_2O, 2% H_2 in Ar	wet	150	0
48	2% N_2O, 2% H_2 in Ar	wet	150	1.50E+04
49	95% N_2, 5% H_2	dry	60	0
50	95% N_2, 5% H_2	dry	60	1.70E+06
51	95% N_2, 5% H_2	dry	90	0
52	95% N_2, 5% H_2	dry	90	1.70E+06
53	95% N_2, 5% H_2	dry	120	0
54	95% N_2, 5% H_2	dry	120	1.70E+06
55	95% N_2, 5% H_2	dry	150	0
56	95% N_2, 5% H_2	dry	150	1.70E+06
57	95% N_2, 5% H_2	wet	60	0
58	95% N_2, 5% H_2	wet	60	1.70E+06
59	95% N_2, 5% H_2	wet	90	0
60	95% N_2, 5% H_2	wet	90	1.70E+06
61	95% N_2, 5% H_2	wet	120	0
62	95% N_2, 5% H_2	wet	120	1.70E+06
63	95% N_2, 5% H_2	wet	150	0
64	95% N_2, 5% H_2	wet	150	1.70E+06
65	10% NH_3 in Ar	dry	60	0
66	10% NH_3 in Ar	dry	60	3.70E+05
67	10% NH_3 in Ar	dry	90	0
68	10% NH_3 in Ar	dry	90	3.70E+05
69	10% NH_3 in Ar	dry	120	0
70	10% NH_3 in Ar	dry	120	3.70E+05
71	10% NH_3 in Ar	dry	150	0
72	10% NH_3 in Ar	dry	150	3.70E+05
73	10% NH_3 in Ar	wet	60	0
74	10% NH_3 in Ar	wet	60	3.70E+05
75	10% NH_3 in Ar	wet	90	0
76	10% NH_3 in Ar	wet	90	3.70E+05
77	10% NH_3 in Ar	wet	120	0
78	10% NH_3 in Ar	wet	120	3.70E+05
79	10% NH_3 in Ar	wet	150	0
80	10% NH_3 in Ar	wet	150	3.70E+05

3.0 Reactions Involving Gases

Gases generated by thermal and radiolytic processes may themselves participate in further reactions. Such reactions might occur in the gas phase within gas bubbles trapped in the waste or might be catalyzed by solid surfaces. Dissolved gases, particularly ammonia, may participate in reactions in the liquid phase. An obvious consequence of such reactions is that gas product distributions can change as a function of the time the gases remain within the wastes. We performed experiments to assess the extent of four sets of reactions under thermal and combined thermal and radiolytic conditions in contact with Tank 241-SY-101 waste simulant. Additional experiments were performed to establish the gas generating capacity of the wet and dried centrifuged solids from the SY1-SIM-92A waste simulant under thermal and radiolytic conditions. The experiments are discussed in the following sections: Section 3.1, gas generation from SY1-SIM-92A waste simulant; Section 3.2, nitrous oxide decomposition reactions; Section 3.3, reactions of nitrous oxide and hydrogen; and Section 3.4, reactions of nitrogen and hydrogen. Ammonia is one of the principal products when nitrous oxide and nitrogen react with hydrogen. A survey of the literature on ammonia decomposition reactions is included in Section 3.5, along with experiments involving reactions of ammonia with Tank 241-SY-101 waste simulant.

3.1 Gas Generation from SY1-SIM-92A Waste Simulant

The gas generation capacity of wet and dried simulated waste solids was evaluated under the same thermal and radiolytic conditions used in previous gas phase reaction studies (Bryan and Pederson 1994, 1995). We did not add organics to this waste simulant because the organics are known to yield high levels of the product gases expected in the present study, possibly masking the result of the gas phase reaction of interest. In addition, we did not expect the organic constituents to catalyze the gas phase reactions significantly nor their omission to affect the intended results.

Gas generation reactions using SY1-SIM-92A were assessed under both thermal-only and combined thermal and radiolytic conditions in the presence of simulated Tank 241-SY-101 waste. A cover gas of argon was used during these tests, which were performed in stainless steel vessels with $\approx$50-mL capacity. Reaction times extended to approximately 70 hours, the reaction temperatures were 60, 90, 120, and 150°C, and radiation dose rates were 0 and 1.7×10^6 R/h. The reaction vessels contained 5 g of simulated waste and were purged with argon after being closed. Gas analyses were performed after each experiment by mass spectrometry. Results for the reaction of the simulated waste solids are shown in Table 3.1 and in Figures 3.1 and 3.2 for the dried and wet solids, respectively.

Gas generation is evident in almost all the reaction systems containing SY1-SIM-92A simulated waste (Figures 3.1 and 3.2). The exception is the thermal-only experiment containing dried simulated waste (Figure 3.1a). Nitrogen is the most prevalent product in both of the combined thermal/radiolytic experiments. In the dried system, the next most abundant gas produced radiolytically is nitrous oxide, followed by other oxides of nitrogen (NO_x). Nitrogen-containing gases are formed from the breakdown of the nitrite and nitrate in the synthetic waste system. This conversion from nitrate and nitrite to N_2, N_2O, and NO_x is radiolytically controlled, since very little of these products is found in the thermal-only reactions with dried SY1-SIM-92A. The radiolytic production of these gases shows a strong thermal component; their concentration increases dramatically with increasing temperature.

Table 3.1. Gas Phase Reaction Compositions of the Thermal and Thermal/Radiolytic Reactions of SY1-SIM-92A (reaction mixtures contained centrifuged wet and dried SY1-SIM-92A simulated waste)

Gas phase composition (mol%), dried SY1-SIM-92A, thermal treatment

Temp, °C	Ar	H_2	N_2	O_2	N_2O	NO_x
60	99.7	0.0095	0.083	0.0172	0.018	0.005
90	99.89	0.001	0.082	0.015	0.015	0.005
120	99.86	0.005	0.086	0.019	0.035	0.005
150	99.73	0.0005	0.084	0.019	0.157	0.01

Gas phase composition (mol%), dried SY1-SIM-92A, thermal and gamma treatment

Temp, °C	Ar	H_2	N_2	O_2	N_2O	NO_x
60	99.27	0.0022	0.127	0.075	0.231	0.005
90	99.2	0.59	0.49	0.076	0.168	0.011
120	98.16	0.137	1.09	0.116	0.39	0.097
150	95.02	0.143	3.09	0.058	1.3	0.38

Gas phase composition (mol%), wet SY1-SIM-92A, thermal treatment

Temp, °C	Ar	H_2	N_2	O_2	N_2O	NO_x
60	99.6	0.001	0.117	0.019	0.008	0.005
90	99.77	0.001	0.158	0.052	0.010	0.01
120	99.43	0.011	0.154	0.054	0.037	0.312
150	95.3	0.048	0.62	0.006	1.99	2.01

Gas phase composition (mol%), wet SY1-SIM-92A, thermal and gamma treatment

Temp, °C	Ar	H_2	N_2	O_2	N_2O	NO_x
60	99.01	0.101	0.83	0.046	0.012	0.005
90	99.07	0.079	0.83	0.12	0.013	0.005
120	98.26	0.302	1.37	0.012	0.046	0.005
150	95.84	0.7	2.46	0.175	0.65	0.16

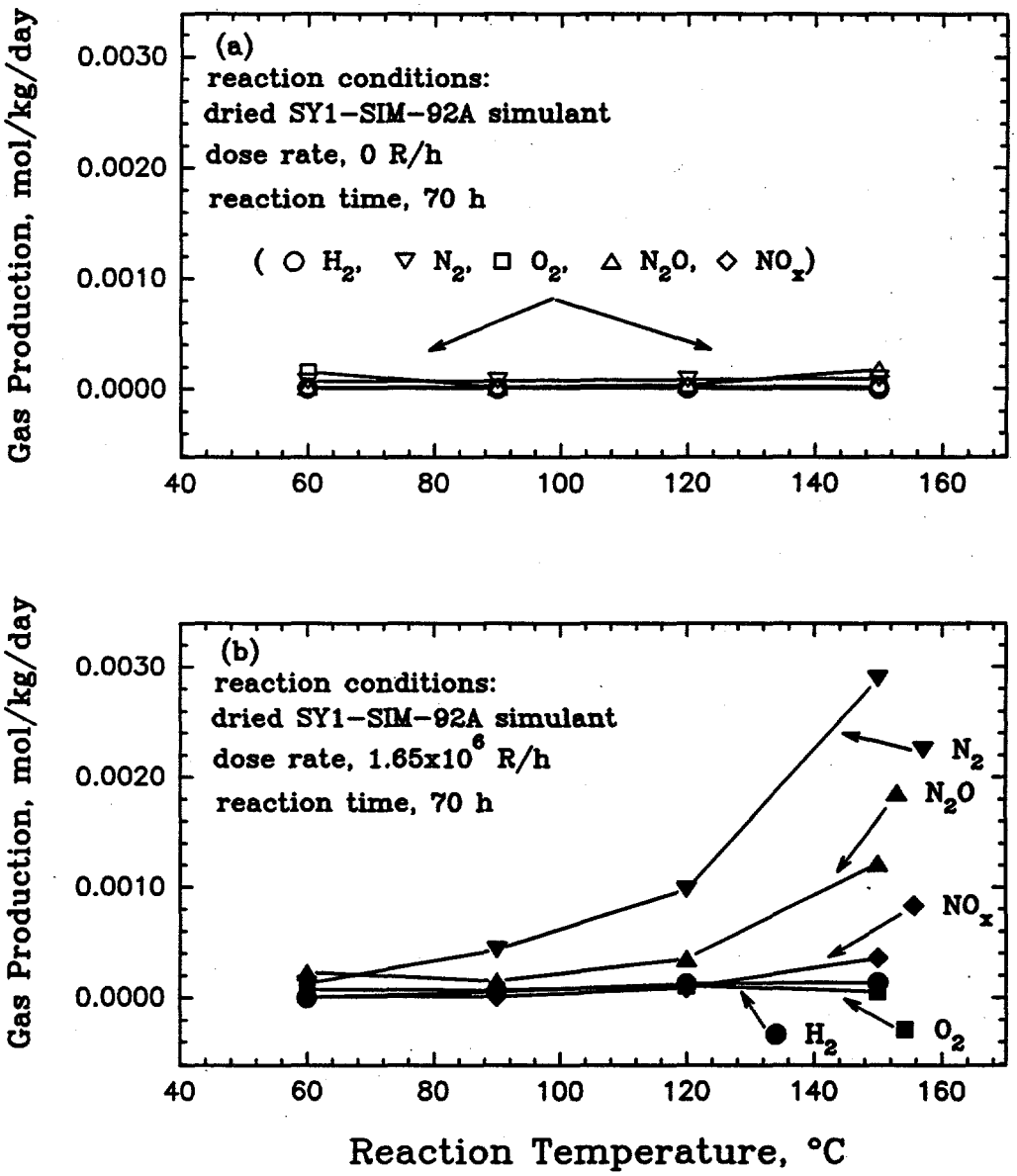

Figure 3.1. Gas Phase Products of Dried SY1-SIM-92A Centrifuged Solids at Termination of Reaction at Various Temperatures

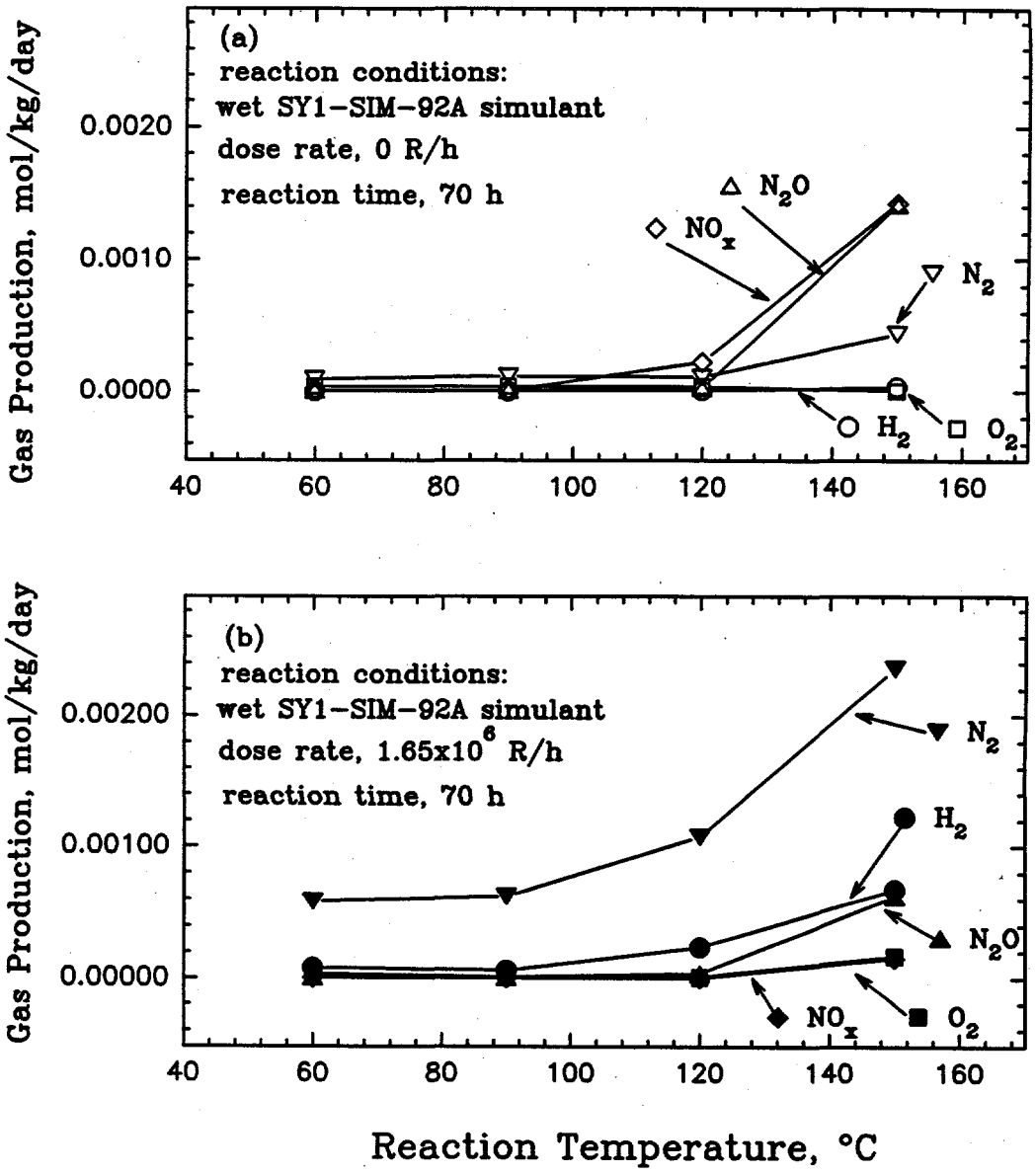

Figure 3.2. Gas Phase Products of Wet SY1-SIM-92A Centrifuged Solids at Termination of Reaction at Various Temperatures

In contrast to the dried simulated waste system, the wet centrifuged solid waste shows hydrogen as the second most abundant radiolytic gas product, followed by nitrous oxide, and then by oxygen and NO_x in trace amounts. The increase in the concentration of hydrogen in the wet system radiolytic reaction (Figure 3.2b) compared with the dry system (Figure 3.1b) is expected, due to the radiolysis of water in this simulant. Higher hydrogen concentrations maybe responsible for lowering the apparent production of nitrous oxide; hydrogen and nitrous oxide are known to react to produce water and nitrogen. The thermal-only experiments with wet simulated waste show an increase in the production of the oxides of nitrogen (N_2O and NO_x) over nitrogen at high temperature. The increase of these oxides of nitrogen in the thermal experiments compared with the radiolytic experiments can be explained by the lack of hydrogen, which would otherwise act as a reductant toward N_2O and NO_x. The reaction of hydrogen with nitrogen oxides can directly form nitrogen as a product. The lack of hydrogen in the thermal-wet reaction system has the effect of reducing the final concentration of nitrogen in these reactions.

G-values for gas generation from SY1-SIM-92A are contained in Table 3.2. These values are based on measurements of gas produced from the thermal and thermal/radiolytic reactions of SY1-SIM-92A. The G-values are calculated as the molecules of gas produced by radiolysis per 100 eV gamma energy absorbed by the entire reaction system. The G-values for nitrogen and nitrous oxide are the highest of the gases produced in the dry simulated waste system; G-values for radiolytic production of NO_x, H_2, and O_2 are relatively small.

Table 3.2.. G-Value Measurements from Radiolytic Gas Generation from SY1-SIM-92A at Various Temperatures (reaction mixture contained centrifuged dried and wet SY1-SIM-92A simulated waste)

Dried SY1-SIM-92A, G-values (molecules/100 eV)

temp, °C	H_2	N_2	O_2	N_2O	NO_x
60	-1.63E-04	1.38E-03	-2.11E-03	5.29E-03	8.64E-06
90	1.30E-03	9.21E-03	1.38E-03	3.44E-03	1.37E-04
120	3.01E-03	2.29E-02	2.20E-03	8.07E-03	2.09E-03
150	3.39E-03	7.13E-02	8.45E-04	2.65E-02	8.78E-03

Wet SY1-SIM-92A, G-values (molecules/100 eV)

temp, °C	H_2	N_2	O_2	N_2O	NO_x
60	2.33E-03	1.45E-02	-6.74E-05	9.85E-05	-4.32E-06
90	1.74E-03	1.50E-02	-8.83E-04	7.95E-05	-1.10E-04
120	6.82E-03	2.87E-02	-8.77E-04	2.80E-04	-6.57E-03
150	1.90E-02	5.71E-02	4.87E-03	-2.35E-02	-3.78E-02

The $G(N_2)$ for nitrogen production in the wet simulated waste is approximately the same as for the dry waste. The $G(H_2)$ for the wet waste is much higher in the wet system as expected owing to the radiolytic production of hydrogen from water in the wet waste. The values for $G(N_2O)$ and $G(NO_x)$ are small and increasingly negative as the temperature increases. The negative G-value arises by the way G-values are calculated. The estimate of the amount of gas formed by the radiolytic reaction alone is calculated as the total formed in the radiolytic reaction at a certain temperature *minus* the amount formed thermally at the same temperature. The negative value for the G-value is interpreted as the thermal formation of these gaseous species followed by the radiolytic decomposition of this compound. Nitrous oxide and NO_x are then either directly decomposed by radiolysis or react directly with a radiolytically produced species (such as the reductants $H\cdot$ or H_2).

The formation of NO_2 and NO (NO_x) in these systems is interesting because these species have not been observed in actual waste from Tank 241-SY-101 (Pederson and Bryan 1994). Oxides of nitrogen may be consumed in reactions with organic carbon, and Tank 241-SY-101 contains approximately 1.5 wt% organics (as wt% total organic carbon [TOC]). There is no organic constituent in these simulated waste systems.

The radiation chemistry of nitrates and nitrites have been studied extensively. Nitrate systems have been shown to yield NO and NO_2 through the radiolytic decomposition of the nitrate ion. The interaction of gamma with nitrate can yield NO_2 directly through the direct effect reaction in the equation below (Meisel et al. 1991):

$$NO_3^- \xrightarrow{\sim\sim} NO_2 + O + e^- \quad (1)$$

The formation of NO_2 and NO can also be accomplished by the solution reaction of NO_3^{2-} and NO_2^{2-} with water according to the following reactions (Muhammad and Maddock 1978):

$$NO_3^{2-} + H_2O \rightarrow NO_2 + 2OH^- \quad (2)$$

$$NO_2^{2-} + H_2O \rightarrow NO + 2OH^- \quad (3)$$

where the formation of NO_3^{2-} and NO_2^{2-} occurs by the interaction of nitrate ion with gamma as follows.

$$2NO_3^- \xrightarrow{\sim\sim} NO_3 + NO_3^{2-} \quad (4)$$

$$3NO_3^- \xrightarrow{\sim\sim} NO_3 + NO_3^{2-} + NO_2^- + O_2 \quad (5)$$

Furthermore, the direct production of NO from the radiolysis of nitrate has been observed by Cunningham (1963) using sensitive chemical analytical methods. The following reaction schemes have been proposed for the direct formation of nitric oxide from nitrate:

$$NO_3^- \xrightarrow{\sim\sim} NO + O_2^- \quad (6)$$

and

$$NO_3^- \xrightarrow{\sim\sim} NO + O^- + O \quad (7)$$

The thermal formation of oxides of nitrogen is of interest as well. Under wet conditions, the simulated waste SY1-SIM-92A produces NO_x, N_2O as well as N_2. Without added organics, the source of the reducing species is not initially apparent. There have been extensive studies of the reduction of nitrate, nitrite, and hydroxylamine using iron(II) as the reductant. The well-known reaction below has been used to form nitrous oxide in an effort to enrich the product gas in ^{15}N with respect to its initial composition (Brown 1966).

$$NO_2^- + Fe(II) \rightarrow NH_2OH \quad (8)$$

$$NH_2OH + NO_2^- \rightarrow N_2O \quad (9)$$

The reaction system used in the current study contains dissolved iron salts (see Table 2.1) and is in contact with a stainless steel reaction vessel. The source of reduced iron for reduction of the nitrite within the system has also been shown to be thermodynamically available when considering the Pourbaix diagram for iron (Pourbaix 1974). Under similar pH conditions in the simulated waste, the Pourbaix diagram for iron species shows that iron would exist as the +2 oxidation state [Fe(II)]. The other nitrogen products (N_2 and NO_x) have been shown to be produced from the thermal decomposition of N_2O under the experimental conditions used in this current work (Johnston 1951; Bryan and Pederson 1995).

3.2 Nitrous Oxide Decomposition Reactions

Nitrous oxide decomposition has been observed in gas generation studies with simulated wastes under both thermal and radiolytic conditions (Ashby et al. 1994b; Bryan and Pederson 1994). Formation of nitrogen gas was enhanced concurrent with the disappearance of nitrous oxide for long reaction times. Such reactions may be important in determining the final proportion of nitrous oxide that is produced in Hanford Site waste tanks. Section 3.2.1 describes the results of measurements to assess the rates of nitrous oxide decomposition in the presence of simulated waste as a function of radiation dose and temperature. Section 3.2.2 includes a literature review of thermal decomposition mechanisms, both gas phase and surface-catalyzed reactions, and compares them with present results. Section 3.2.3 addresses radiolytic mechanisms.

3.2.1 Nitrous Oxide Decomposition Experimental Results

Nitrous oxide decomposition reactions in the presence of simulated waste were assessed under thermal and combined thermal and radiolytic conditions. Reactions were conducted in stainless steel vessels in the temperature range of 60 to 150°C and gamma radiation doses of 0 and 10^7 rad; reaction times extended to approximately 150 hours. The reaction vessels were initially filled with nitrous oxide at one atmosphere total pressure. Gas compositions were analyzed by mass spectrometry before and after the tests.

The decomposition of nitrous oxide was apparent for the reaction systems containing dry and wet SY1-SIM-92 waste simulant, in both thermal only and thermal/radiolytic conditions, over the temperature range 60 to 150°C. The data are contained in Tables 3.3 and 3.4 and shown in Figures 3.3 and 3.4 for the reaction of nitrous oxide in the presence of dried and wet simulated waste, respectively.

Table 3.3.. Gas Phase Compositions of Nitrous Oxide Decomposition Reactions (reaction mixture contained dried SY1-SIM-92A simulated waste)

Gas Composition, mol%						
N_2O	N_2	O_2	H_2	NO_x	Dose (R)	Conditions
98.69	0.353	0	0.0074	0.87	0	60°C, dried SY1-SIM-92A
98.29	0.82	0	0.0065	0.83	1.24E+07	60°C, dried SY1-SIM-92A
99.72	0.178	0.01	0.002	0.017	0	90°C, dried SY1-SIM-92A
98.35	1.47	0.032	0.003	0.008	2.59E+07	90°C, dried SY1-SIM-92A
98.75	0.37	0.0011	0.0057	0.81	0	120°C, dried SY1-SIM-92A
98.4	0.84	0	0.0092	0.71	1.24E+07	120°C, dried SY1-SIM-92A
98.6	0.39	0	0.0047	0.92	0	150°C, dried SY1-SIM-92A
98	0.85	0.0039	0.03	1.1	1.23E+07	150°C, dried SY1-SIM-92A

Table 3.4. Gas Phase Compositions of Nitrous Oxide Decomposition Reactions (reaction mixture contained centrifuged wet SY1-SIM-92A simulated waste)

Gas Compositions, mol %						
N_2O	N_2	O_2	H_2	NO_x	Dose (R)	Conditions
98.9	0.71	0.089	0.11	0.275	0	60°C; wet SY1-SIM-92A
98.5	1.13	0.038	0.01	0.247	1.24E+07	60°C; wet SY1-SIM-92A
99.85	0.066	0.019	0.0033	0.01	0	90°C; wet SY1-SIM-92A
98.88	1	0.023	0.0017	0.01	2.40E+07	90°C; wet SY1-SIM-92A
99.22	0.292	0	0.008	0.451	0	120°C; wet SY1-SIM-92A
98.86	0.74	0	0.005	0.384	1.24E+07	120°C; wet SY1-SIM-92A
99.63	0.151	0	0.0075	0.168	0	150°C; wet SY1-SIM-92A
99.11	0.85	0	0.003	0.012	1.23E+07	150°C; wet SY1-SIM-92A

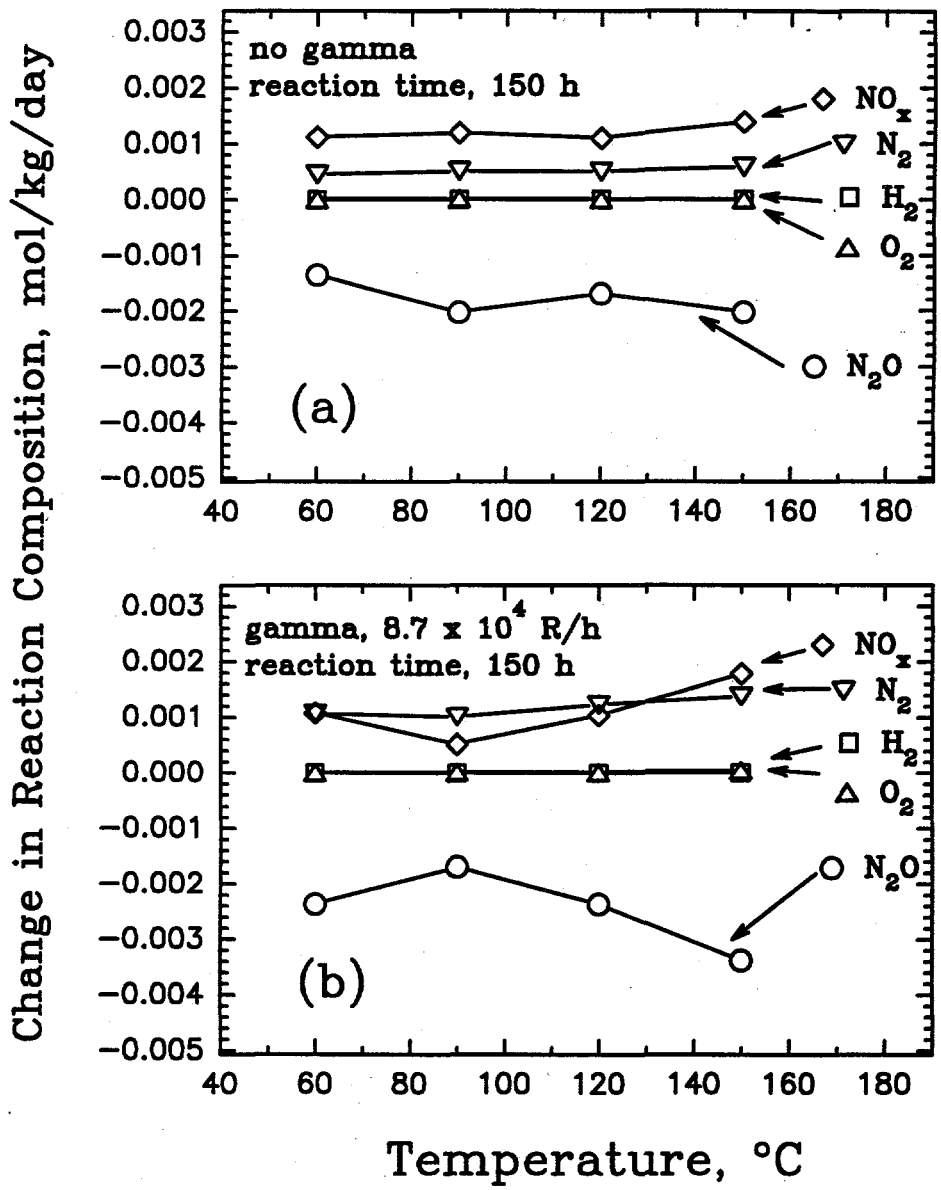

Figure 3.3. Gas Phase Composition of Nitrous Oxide in Contact with Dried SY1-SIM-92A Centrifuged Solids at Termination of Reaction at Various Temperatures

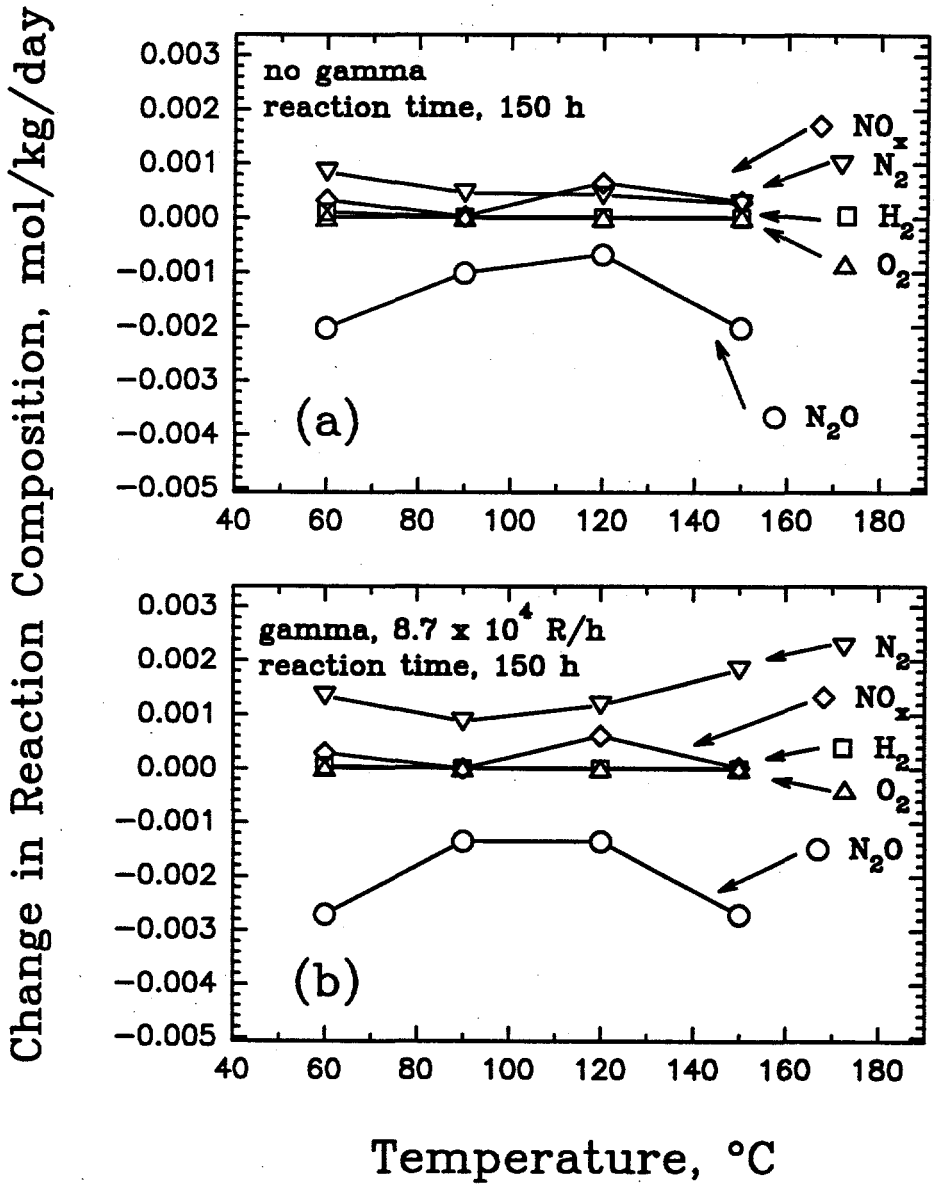

Figure 3.4. Gas Phase Composition of Nitrous Oxide in Contact with Wet SY1-SIM-92A Centrifuged Solids at Termination of Reaction at Various Temperatures

For nitrous oxide in contact with dried solids, a greater amount of N_2O reacted in the irradiated sample (Figure 3.3b) than in the thermal-only sample (Figure 3.3a). The disappearance of nitrous oxide showed similar temperature behavior in both the radiolytic and thermal-only experiments with wet solids (Figures 3.4a and b respectively); a greater amount of nitrous oxide was reacted in the radiolytic experiment than in the thermal-only experiment. As can be seen in Figure 3.3a, the reaction of nitrous oxide under thermal-only conditions shows only a slight temperature dependence for the change in moles of nitrous oxide reactant. The data are displayed in change of reactant or product per kg waste per day (mol/kg/day) as a function of reaction temperature.

The reactions containing wet simulated waste in both the radiolytic and thermal-only experiments have nitrogen as their main product, followed by NO_x. The production of nitrogen is more evident in the radiolytic experiment, which corresponds to the increased consumption of nitrous oxide in the radiolytic reactions. The production of hydrogen and oxygen are insignificant in these reactions.

The reactions containing dried simulated waste have NO_x as the most abundant product for the thermal only reactions, followed by nitrogen. In the radiolytic experiments, the production of NO_x and nitrogen are approximately equal but change in dominance from 60 to 150°C. As in the wet simulated solids reactions, production of hydrogen and oxygen is relatively insignificant.

In contrast, no nitrous oxide decomposition was observed without gamma ray irradiation in the absence of simulated waste in the temperature range of 60 to 150°C (Bryan and Pederson 1995). Decomposition under radiolytic conditions was apparent, at rates that increased with increased radiation dose. The extent of radiolytic decomposition of nitrous oxide in the absence of simulated waste showed no discernable temperature dependence, as can be seen from the data in Figure 3.5 (from Bryan and Pederson 1995).

Although the rate of the nitrous oxide decomposition in the absence of simulated waste appeared to be independent of temperature for a given radiation dose, the distribution of the products of decomposition was somewhat temperature-sensitive (Bryan and Pederson 1995). Products of decomposition were nitrogen, oxygen, and nitrogen dioxide. In particular, NO_x concentrations were highest at 60°C and decreased with increased temperature. Nitrogen yields were inversely related to those of nitrogen dioxide, as expected. Calculated radiolytic yields (G-values) for each of the products and the reactant are summarized here in Table 3.5 for each experimental condition. G-values are also given in Figure 3.5 as a function of temperature, where the approximately inverse relation between nitrogen and NO_x yields can be seen.

When we compare the quantity of nitrous oxide decomposed in the gas phase reaction (Bryan and Pederson 1995) with the quantity of nitrogen-containing compounds formed (molecular nitrogen plus nitrogen dioxide), we come up short, especially at the lowest temperatures. At higher temperatures where little nitrogen dioxide was detected, the nitrogen mass balance was quite good. The oxygen mass balance was poor, presumably because it was consumed in reactions with the vessel. Nitrous oxide and nitrogen concentrations are the least subject to bias. At high temperatures (150°C), the quantities of nitrogen formed and nitrous oxide decomposed were reported to be equal on a molar basis, within experimental scatter.

Table 3.5. G-Value Measurements for Decomposition of N_2O at 60°, 90°, 120°, and 150°C

G-Value (molecule/100 eV) $G(N_2O)$	$G(N_2)$	$G(O_2)$	$G(NO_x)$	Conditions	Dose
-12.0	7.33	1.3	3.5	60°C	6.84×10^6
-10.6	11.2	1.1	0.5	90°C	6.47×10^6
-12.8	11.0	0.7	-1.8	120°C	6.47×10^6
-12.9	14.5	0.3	0.0	150°C	6.42×10^6
-12	8.1	1.1	3.9	Room temp	$<10^9$ [a]

(a) G-values measured at room temperature, dose $<10^9$ R. Data taken from Harteck and Dondes (1956).

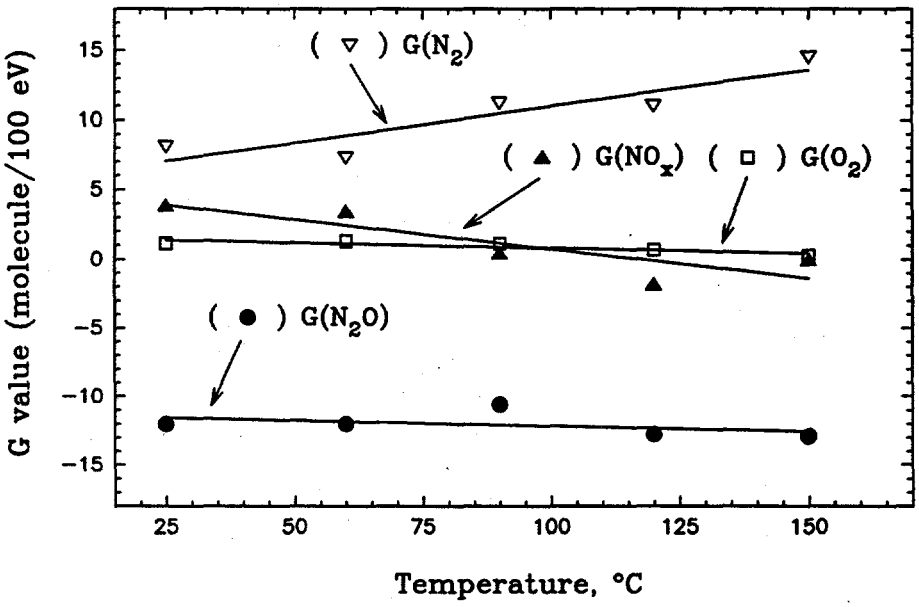

Figure 3.5. G-Value Measurements for Decomposition of N_2O at Room Temperature, 60, 90, 120, and 150°C

The G-value for the decomposition of nitrous oxide becomes less negative with increasing temperature from 60 to 150°C for the wet centrifuged solids in contact with nitrous oxide and from 60 to 120° for the dried solids reaction system, indicating that the thermal pathway for the decomposition of nitrous oxide may be becoming more dominant with increasing temperature. The G-values for nitrous oxide decomposition and product formation in the presence of dried and wet simulated waste are presented in Tables 3.6 and 3.7, respectively. The G-value data are also displayed in Figures 3.6 and 3.7 for the wet and dried simulated waste reaction systems, respectively. For the dried centrifuged solids system, the G-value for the decomposition of nitrous oxide is much more negative at 150°C than at lower temperatures. Although the sharp increase in nitrous oxide decomposition at 150°C is not easily explained, the surface catalyzed decomposition of nitrous oxide will become more important at higher temperatures. At this temperature, the G-value for the production of NO_x increases to offset the increase in the nitrous oxide decomposition.

In the wet centrifuged solids system, the G-value for NO_x is essentially zero; when it reaches 150°C it becomes significantly negative. Since there is no NO_x present at the start of these reactions, the negative value for $G(NO_x)$ is interpreted as a thermal generation of NO_x followed by a radiolytic decomposition of this species. Concurrent with the radiolytic NO_x decomposition, the value for $G(N_2)$ increases dramatically at 150°C in these reactions. An inverse relationship between NO_x decomposition and the appearance of nitrogen was observed by Bryan and Pederson (1995).

Table 3.6. G-Value Measurements for Decomposition of Nitrous Oxide in Contact with Dried SY1-SIM-92A Simulated Waste

G-Value (molecule/100 eV)						
N_2O	N_2	O_2	H_2	NO_x	Dose (R)	Conditions
-14.35	8.66	0	-0.015	-0.57	1.24E+07	60°C; dried SY1-SIM-92A[a]
-4.69E-01	2.83E-01	0	-5.00E-04	-1.88E-02	1.24E+07	60°C; dried SY1-SIM-92A[b]
-11.37	11.34	0.19	0.0088	-0.079	2.59E+07	90°C; dried SY1-SIM-92A[a]
-3.40E-01	3.34E-01	5.69E-03	2.59E-04	-2.33E-03	2.59E+07	90°C; dried SY1-SIM-92A[b]
-8.46	9.18	-0.019	0.0719	-0.72	1.24E+07	120°C; dried SY1-SIM-92A[a]
-3.11E-01	3.38E-01	-6.87E-04	2.65E-03	-2.65E-02	1.24E+07	120°C; dried SY1-SIM-92A[b]
-17.05	10.06	0.08	0.528	5.07	1.23E+07	150°C; dried SY1-SIM-92A[a]
-6.25E-01	3.69E-01	2.94E-03	1.94E-02	1.86E-01	1.23E+07	150°C; dried SY1-SIM-92A[b]

(a) G-value calculation based on mass of gas phase only.
(b) G-value calculation based on total mass of system.

Table 3.7. G-Value Measurements for Decomposition of Nitrous Oxide in Contact with Centrifuged, Wet SY1-SIM-92A Simulated Waste

G-Value (molecule/100 eV)						
N_2O	N_2	O_2	H_2	NO_x	Dose (R)	Conditions
-10.35	7.76	-0.9209	-0.0166	-0.476	1.24E+07	60°C; wet SY1-SIM-92A[a]
-3.03E-01	2.35E-01	-2.79E-02	-5.06E-04	-1.44E-02	1.24E+07	60°C; wet SY1-SIM-92A[b]
-8.77	8.82	0.0378	-0.0151	3.97E-05	2.40E+07	90°C; wet SY1-SIM-92A[a]
-2.58E-01	2.60E-01	1.00E-03	-4.45E-04	1.17E-06	2.40E+07	90°C; wet SY1-SIM-92A[b]
-7.82	8.79	0	-0.0403	-0.391	1.24E+07	120°C; wet SY1-SIM-92A[a]
-3.10E-01	3.49E-01	0	-1.60E-03	-1.55E-02	1.24E+07	120°C; wet SY1-SIM-92A[b]
-7.87	18.22	0	-0.0791	-3.158	1.23E+07	150°C; wet SY1-SIM-92A[a]
-3.08E-01	7.13E-01	0	-3.10E-03	-1.24E-01	1.23E+07	150°C; wet SY1-SIM-92A[b]

(a) G-value calculation based on mass of gas phase only.
(b) G-value calculation based on total mass of system.

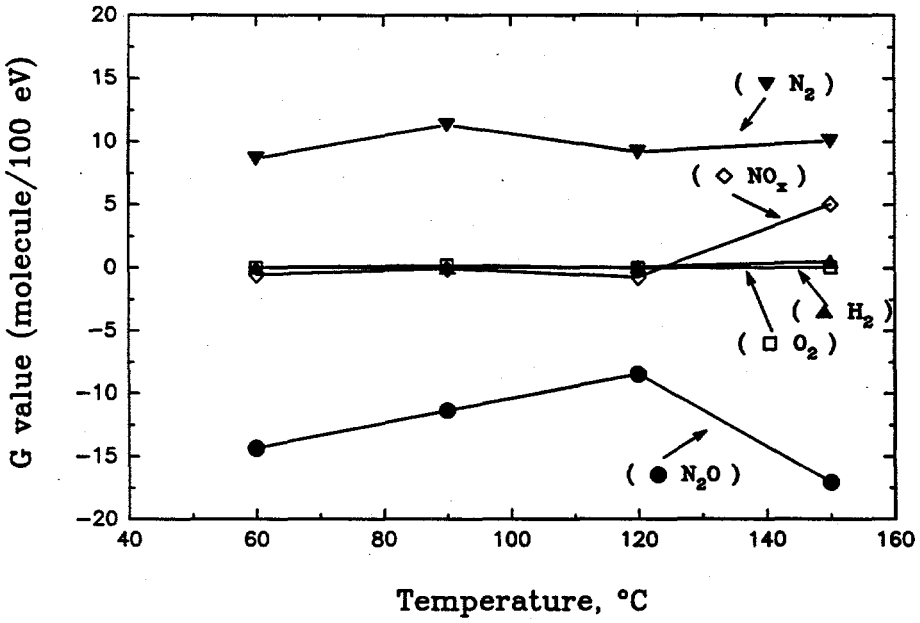

Figure 3.6. G-Value Measurements for the Reaction of Nitrous Oxide in Contact with Dried Centrifuged SY1-SIM-92A Solids

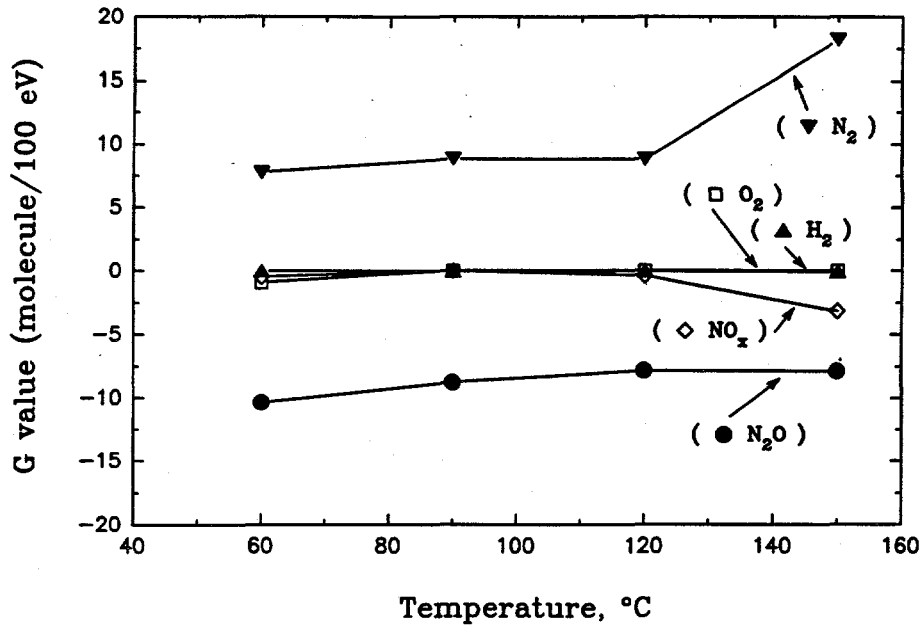

Figure 3.7. G-Value Measurements for the Reaction of Nitrous Oxide in Contact with Wet Centrifuged SY1-SIM-92A Solids

3.2.2 Thermal Decomposition of Nitrous Oxide: Literature Review and Discussion

Nitrous oxide can decompose thermally by a complex reaction in the gas phase or by surface-catalyzed reactions. Homogeneous unimolecular gas-phase reactions are expected to be far too slow to be of any importance at Hanford tank waste temperatures (< 100°C). Solid surface-catalyzed reactions may result in altered gas product yields in the tank wastes, however.

The kinetics of decomposition of nitrous oxide under thermal conditions in the gas phase has been widely studied (Johnston 1951; Lindars and Hinshelwood 1955a, 1955b; Kaufman et al. 1956; Preston and Cvetanovic 1972). Reactions occur following Johnston (1951):

$$N_2O \rightarrow N_2 + O \quad (10)$$

$$O + N_2O \rightarrow N_2 + O_2 \quad (11)$$

$$O + N_2O \rightarrow 2\ NO \quad (12)$$

Reaction (11) predominates over Reaction (12) below approximately 400K, while the reverse is true above that temperature (Johnston 1951; Kaufman et al. 1956; Preston and Cvetanovic 1972).

Decomposition of nitrous oxide has been described by a first-order rate expression (Johnston 1951; Laidler 1965):

$$-d[N_2O]/dt = k\,[N_2O] \quad (13)$$

Linders and Hinshelwood (1955a, 1955b) have found that nitrous oxide decomposition kinetics deviate from first-order behavior, depending on the partial pressure of nitrous oxide and the presence of other gases. Rate coefficient data corresponding to Equation (13) that was given by Johnston (1951) is believed sufficient to estimate nitrous oxide decomposition rates in the gas phase, however:

$$k = 4.4 \times 10^{11} \exp[-60{,}000/RT] \quad (14)$$

where k has units of s^{-1}, R is the gas constant, 1.9872 cal/K-mol, and T is temperature (K). Equation (14) corresponds to data obtained in the temperature range 900 to 1050K, well above temperatures applicable to gas generation studies. Activation energies determined in other studies ranged from approximately 50 to 60 kcal/mole, with pre-exponential factors ranging from 10^{10} to nearly 10^{13} s^{-1}, as summarized by Preston and Cvetanovic (1972).

Clearly, the homogeneous unimolecular decomposition of nitrous oxide is unimportant at temperatures relevant to tank wastes. Following Equation (14) and approximately first-order rate behavior, more than 10^{18} years would be required for 1% of the nitrous oxide to decompose at 60°C. At 120°C, more than 10^{12} years would be required. Temperatures of 400°C or higher are predicted to be required to decompose 1% of the original nitrous oxide concentration within 1000 hours by this mechanism. Present data are consistent with this assessment, showing no measurable decomposition under thermal-only conditions.

Nitrous oxide decomposition reactions can be strongly affected by interactions with solids. These interactions result in lowering the activation energy for decomposition by approximately a factor of two. Hinshelwood and Pritchard (1925a) determined an activation energy of 29.0 kcal/mole for the heterogeneous decomposition of nitrous oxide on a gold surface; the activation energy determined for this reaction was 32.5 kcal/mole for a platinum surface (Hinshelwood and Pritchard 1925b), 34.8 kcal/mole for a calcium oxide surface and 29.3 kcal/mole for an aluminum oxide surface (Schwab, Stager, and von Baumbach 1933).

A variety of metal oxide catalysts have been shown to be effective in catalyzing nitrous oxide decomposition as well. The effectiveness of oxide catalysts is as follows: $Cu_2O > CoO > NiO > MgO > CaO > Al_2O_3 > ZnO > CdO > TiO_2 > Cr_2O_3 > Fe_2O_3 > Ga_2O_3$ (Wagner and Hauffe 1938; Garner, Gray, and Stone 1950; Hauffe, Glang, and Engell 1950; Engell and Hauffe 1953; Dell, Stone, and Tiley 1953). Surface-catalyzed reactions have been proposed to follow this sequence (Wagner and Hauffe 1938):

$$N_2O + e\ (\text{from surface}) \rightarrow N_2 + O^-_{ads} \quad (15)$$

$$O^-_{ads} \rightarrow 1/2\ O_2 + e \quad (16)$$

$$O^-_{ads} + N_2O \rightarrow N_2 + O_2 + e\ (\text{to surface}) \quad (17)$$

where O^-_{ads} is a surface-adsorbed oxygen ion. Catalysts that are p-type (excess electron holes) are found to be the best catalysts for this reaction; catalysts that are n-type (excess electrons) are the poorest, while insulators are intermediate.

Heterogeneous reactions are expected to be of greatest relative importance at low temperatures (Laidler 1965). The velocity of a homogeneous unimolecular reaction is, according to absolute reaction rate theory,

$$\upsilon_{hom} = c_A\,[kT/h]\,[F_+/F_A]\,\exp[-E_{hom}/RT] \tag{18}$$

while that of a heterogeneous, surface-catalyzed reaction is

$$\upsilon_{het} = c_A\,c_S\,[kT/h]\,[1/F_A]\,\exp[-E_{het}/RT] \tag{19}$$

where c_A and c_S are concentrations of nitrous oxide in the gas phase and on a solid surface, respectively, E_{hom} and E_{het} are activation energies for homogeneous and heterogeneous reactions, respectively, and F_+ and F_A are partition functions for the activated complex and for nitrous oxide in the gas phase, respectively. Dividing Equation (19) by Equation (18), one obtains

$$\upsilon_{het}/\upsilon_{hom} = c_S/F_+\,\exp[\Delta E/RT] \tag{20}$$

where ΔE is $E_{hom} - E_{het}$. For 1 cm^2 of solid surface area, the term c_S is approximately 10^{15}, whereas for 1 cm^3 of nitrous oxide gas, F_+ is approximately 10^{27}. Following the above discussion, ΔE is approximately 30 kcal/mole for nitrous oxide reactions. Thus we have

$$\upsilon_{het}/\upsilon_{hom} \approx 10^{-12}\,\exp[30{,}000/RT] \tag{21}$$

From Equation (21), which is based on absolute rate theory, heterogeneous reactions are predicted to dominate at temperatures less than about 300°C. Of course, actual reaction rates may vary widely, depending on the catalytic properties of the solid surface. It can be concluded that any experimental observation of nitrous oxide decomposition at temperatures relevant to waste storage must be due to surface-mediated reactions, not to true gas-phase reactions.

Nitrous oxide decomposition in glass reaction vessels has been attributed to catalysis by the glass walls in studies conducted by Ashby et al. (1994b). Nitrous oxide decomposition catalyzed by glass surfaces has long been recognized (Hibben 1928; Lindars and Hinshelwood 1955a). Experiments of Ashby et al. (1994b) were conducted at 120°C in glass reaction vessels for approximately 1000 hours. The first-order rate constant determined was approximately 10^{-7} s^{-1}, whether simulated waste mixtures were present in the reaction vessel or not. This rate constant is many orders of magnitude larger than expected from Equation (14). Ashby et al. (1994b) noted that the above rate constant has meaning only for a particular apparatus that was used, because the value depends on the glass surface-area-to-gas-volume ratio. Rates may also be expected to vary with the surface composition of the glass vessel, which may change with age and use.

That stainless steel used in the present studies would have little influence on nitrous oxide decomposition rates is not unexpected. The surface of the stainless steel is expected to be high in chromium oxide and iron oxide (Baer and Dake 1986; Briant and Mulford 1982). Oxides of iron and chromium are known to be poor catalysts for this reaction (Wagner and Hauffe 1938; Garner, Gray, and Stone 1950; Hauffe, Glang, and Engell 1950; Engell and Hauffe 1953; Dell, Stone, and Tiley 1953). In contrast, Ashby et al. (1994b) found that nitrous oxide was thermally decomposed in glass vessels under otherwise similar conditions. While the type of glass used was not identified, compositions

typically used in laboratory glassware include silica, alumina, boron oxide, sodium oxide, calcium oxide, magnesium oxide, and other components (Doremus 1973). As discussed above, aluminum oxide and the alkaline earth oxides have been found to be more effective catalysts than the oxides of iron or chromium for nitrous oxide decomposition.

In the Hanford waste tanks, the steel walls are expected to contribute negligibly to nitrous oxide decomposition. Not only is the expected catalytic activity of the steel for this reaction quite low, but the tank surface-area-to-volume ratio is very small. Gases trapped as bubbles in the sludge will not contact the steel tank walls. Once released to the plenum space above the wastes, the gases will be removed through the ventilation system in a relatively short time.

Catalysis of nitrous oxide decomposition by solid phases present in the waste is a significant possibility, however. At least some of the gases will be retained as bubbles attached to solid particles, in response to surface tension forces (Bryan, Pederson, and Scheele 1992). Thus the gases will be in intimate contact with tank solids, which include sodium aluminate, sodium nitrate, sodium nitrite, sodium carbonate, and other phases (Herting et al. 1992a, 1992b). The results of this study show that catalysis of nitrous oxide decomposition by such solids is a possibility. The temperature dependence of the G-value for the decomposition of nitrous oxide in the presence of wet or dried waste simulant solids shows that a thermal component is involved. By contrast, the gas phase reaction showed no thermal sensitivity over the same temperature range (Bryan and Pederson 1995). In addition, the thermal reaction of nitrous oxide in the presence of simulated waste solids showed significant conversion of nitrous oxide to other gas products (Tables 3.2 and 3.3, Figures 3.3 and 3.4), while under similar conditions, the gas phase reaction showed no conversion under thermal conditions alone (Bryan and Pederson 1995).

In thermal reactions in the presence of wet centrifuged solids, between 0.4 to 1.1% of the nitrous oxide was decomposed thermally after 150 hours. For the dried simulated waste experiment the rate of nitrous oxide decomposition was higher—approximately 1.25 to 1.5% decomposed over the same time period. Based on these data, and assuming a pseudo-zero order, surface catalyzed reaction can be estimated to decompose between $\approx$20 to $\approx$90% of the nitrous oxide in one year.

3.2.3 Radiolytic Decomposition of Nitrous Oxide: Literature Review and Discussion

The radiation chemistry of nitrous oxide is complex, and the complete mechanism of reaction has not been fully developed (Spinks and Woods 1990). Nitrous oxide finds use as a gas-phase dosimeter (Johnson 1973) and as an electron scavenger (Harteck and Dondes 1956). Products of radiolytic reactions of nitrous oxide include nitrogen, oxygen, and nitric oxide; G-values for these products are 1.04 ± 0.02, 0.41 ± 0.04, and 0.41 ± 0.04 μmoles, respectively, or 10.0, 3.9, and 3.9 molecules/100 eV, respectively (Spinks and Woods 1990).

Radiolytic yields obtained in this study for nitrous oxide decomposition, at relatively low total doses, are in excellent agreement with literature values (Harteck and Dondes 1956; Simpson 1961), as shown in Table 3.4. Literature values and present results were in agreement although present measurements were made at temperatures from 60 to 150°C while literature results were obtained at 25°C. This finding emphasizes the lack of temperature dependence for radiolytic reactions of nitrous oxide.

This finding emphasizes the lack of temperature dependence for radiolytic reactions of nitrous oxide. But at higher radiation doses ($\approx 1.7 \times 10^8$ R), measured G-values deviated substantially from literature values. Harteck and Dondes (1956) noted that G-values for nitrous oxide decomposition were not constant above total doses of 10^9 R due to secondary reactions of the initial products.

Nitric oxide will react instantly with oxygen to form nitrogen dioxide, following Cotton and Wilkinson (1980):

$$2\ NO + O_2 \rightarrow 2\ NO_2 \qquad (22)$$

If water vapor is present, nitrogen dioxide will react with water to yield nitric acid and nitric oxide, a reaction that is used widely on an industrial scale. Another reaction of potential importance in the waste tanks is the reaction of nitrogen dioxide, water vapor, and ammonia to yield ammonium nitrate (Bou-Hamra 1988; Pederson and Bryan 1994), which also is used on an industrial scale. In Tank 241-SY-101, however, which is closely monitored by infrared spectrometry and other probes, neither nitrogen dioxide nor nitric oxide been observed, nor have ammonium nitrate solids been detected (see Pederson and Bryan 1994 and references therein).

Thermodynamically unstable, nitric oxide will decompose to yield nitrous oxide and nitrogen dioxide following Cotton and Wilkinson (1980):

$$3\ NO \rightarrow N_2O + NO_2 \qquad (23)$$

Equation (14) is important only for high nitric oxide pressures where collisions between NO molecules are more probable (Melia 1965) and should be of little importance in Hanford Site waste tanks.

Among gases likely to be formed in the Hanford Site waste tanks, nitrous oxide is unique in its ability to capture electrons, following (Spinks and Woods 1990):

$$e^- + N_2O \rightarrow N_2 + O^- \qquad (24)$$

Oxygen ions can then react further with nitrous oxide molecules:

$$O^- + N_2O \rightarrow NO^- + NO \qquad (25)$$

The ionic species NO^- will decompose to yield NO and an electron, which can then react following Equation (24). In aqueous systems, nitrous oxide is effective in scavenging hydrated electrons to yield hydroxyl radicals and nitrogen gas. However, this reaction is overshadowed by hydrated electron scavenging by the nitrate ion in Hanford Site tank wastes (Meisel et al. 1993).

The extent of nitrous oxide decomposition due to gas phase radiolytic reactions is readily estimated. Assuming a gamma dose rate in the wastes of $\approx 10^3$ R/h, a value of $G(-N_2O)$ of -12 molecules/100 eV (Harteck and Dondes 1956), and a gas mixture of 30% nitrous oxide, 30% nitrogen, 30% hydrogen, and 10% ammonia, it is estimated that 0.9% of the nitrous oxide will decompose each year. Thus the impact of nitrous oxide radiolysis in the gas phase on gas product distributions is expected to be relatively minor.

3.3 Reactions of Nitrous Oxide and Hydrogen

Nitrous oxide and hydrogen are two of the principal gases produced by thermal and radiolytic reactions in Tank 241-SY-101; each accounts for approximately 30 mole percent of the total (LANL 1994). Nitrous oxide and hydrogen are known to react to produce ammonia, nitrogen, oxygen, and water, depending on conditions. Experimental results on thermal and combined thermal and radiolytic reactions of nitrous oxide and hydrogen reactions in the presence of simulated waste are described in Section 3.3.1. In Section 3.3.2, thermally driven reactions of nitrous oxide are discussed, including a survey of the literature and comparison to present results. Section 3.3.3 addresses nitrous oxide and hydrogen reactions under combined radiolytic and thermal conditions.

3.3.1 Experimental Results for Nitrous Oxide and Hydrogen Reactions

Reactions of nitrous oxide and hydrogen were probed under thermal and combined thermal and radiolytic conditions in $\approx$500-mL stainless steel vessels. Reaction times extended to $\approx$150 hours, reaction temperatures were 60, 90, 120, and 150°C, and radiation dose rates were 0 and 1.5×10^4 R/h. Initial concentrations of N_2O and H_2 gases were intentionally kept at approximately 2 mole percent to ensure that the mixture did not exceed the lower flammability limit. An inert gas (argon) was added as a diluent at an approximate concentration of 96 mole percent for that purpose.

In earlier studies it was found that under thermal-only conditions, the principal products of the gas phase reaction of nitrous oxide with hydrogen were nitrogen, oxygen, water, and a very small concentration of ammonia (Bryan and Pederson 1995). Under combined thermal and radiolytic conditions, while similar products were found as in thermal-only conditions, the extent of nitrous oxide and hydrogen consumption and ammonia formation was considerably greater.

Similar trends are observed for the reaction of nitrous oxide with hydrogen in contact with simulated waste and for the reaction of these gases in the gas phase alone. The primary product of the reaction of nitrous oxide with hydrogen in contact with dried or wet simulated waste is nitrogen, followed by oxygen and other oxides of nitrogen. The gas phase components of these reactions is shown in Tables 3.8 and 3.9, and the change in gaseous products and reactants (mol/kg/day) is displayed in Figures 3.8 and 3.9. The production of nitrogen and oxygen increased considerably with irradiation compared with the experiments performed under thermal conditions alone. The decomposition of hydrogen and nitrous oxide was temperature-dependent, especially in the irradiated sample in contact with wet simulated waste (Figure 3.9b). Nitrogen production increases with increasing temperature following the consumption of nitrous oxide in these reactions.

For all of the reactions of nitrous oxide with hydrogen in contact with dried or wet simulated waste, the mass balance for gas-phase nitrogen was not good. The gain in nitrogen is more than can be accounted for by the loss of nitrous oxide alone, most likely due to the production of nitrogen from the solid phase sources of nitrogen, nitrite and nitrate. These solid phase reactants have been shown to produce nitrogen under similar temperature and irradiation conditions with simulated wastes (Bryan and Pederson 1994; Bryan et al. 1992).

Table 3.8. Gas Phase Compositions of Nitrous Oxide and Hydrogen Reactions Under Thermal and Radiolytic Conditions (mixture contained dried SY1-SIM-92A simulated waste)

Gas Compositions, mol %							
N_2O	N_2	O_2	H_2	NO_x	Ar	Dose (R)	Conditions
2.02	0.155	0.224	2.05	0.007	95.7	0	60°C, dried SY1-SIM-92A
1.91	0.313	0.033	1.92	0.005	95.8	4.65E+06	60°C, dried SY1-SIM-92A
1.99	0.170	0.004	1.97	0.015	95.8	0	90°C, dried SY1-SIM-92A
1.87	0.303	0.023	1.91	0.01	95.9	4.62E+06	90°C, dried SY1-SIM-92A
2.01	0.154	0.003	1.99	0.02	95.81	0	120°C, dried SY1-SIM-92A
1.88	0.314	0.02	1.91	0.012	95.81	4.64e+06	120°C, dried SY1-SIM-92A
1.98	0.425	0.016	1.87	0.009	95.68	0	150°C, dried SY1-SIM-92A
1.95	0.510	0.011	1.81	0.11	95.60	4.64e+06	150°C, dried SY1-SIM-92A

Table 3.9. Gas Phase Compositions of Reaction of Nitrous Oxide and Hydrogen Under Thermal and Radiolytic Conditions (mixture contained centrifuged, wet SY1-SIM-92A simulated waste)

Gas Compositions, mol %							
N_2O	N_2	O_2	H_2	NO_x	Ar	Dose (R)	Conditions
2.01	0.361	0.021	2.05	0.002	95.6	0	60°C; wet SY1-SIM-92A
1.93	0.472	0	1.95	0	95.1	4.65E+06	60°C; wet SY1-SIM-92A
2.03	0.211	0.002	2	0.004	95.8	0	90°C; wet SY1-SIM-92A
1.87	0.367	0.022	1.85	0.002	95.9	4.62E+06	90°C; wet SY1-SIM-92A
2.02	0.215	0	1.96	0.003	95.8	0	120°C; wet SY1-SIM-92A
1.72	0.51	0.007	1.77	0	96	5.01E+06	120°C; wet SY1-SIM-92A
2.04	0.246	0.001	1.93	0.339	95	0	150°C; wet SY1-SIM-92A
1.83	0.52	0.005	1.82	0	95.8	4.65E+06	150°C; wet SY1-SIM-92A

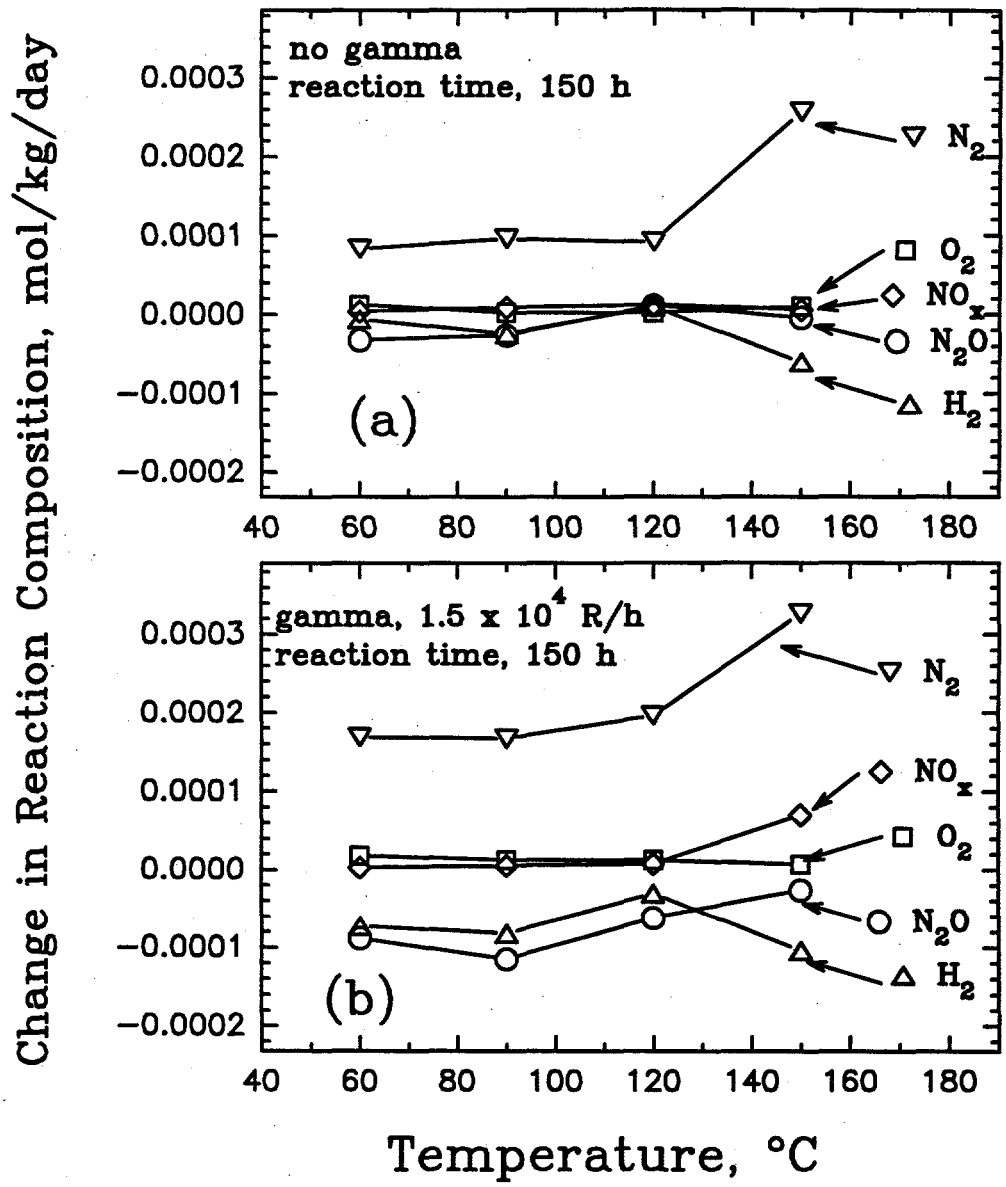

Figure 3.8. Gas Phase Composition of Hydrogen and Nitrous Oxide in Contact with Dried SY1-SIM-92A Centrifuged Solids at Termination of Reaction at Various Temperatures

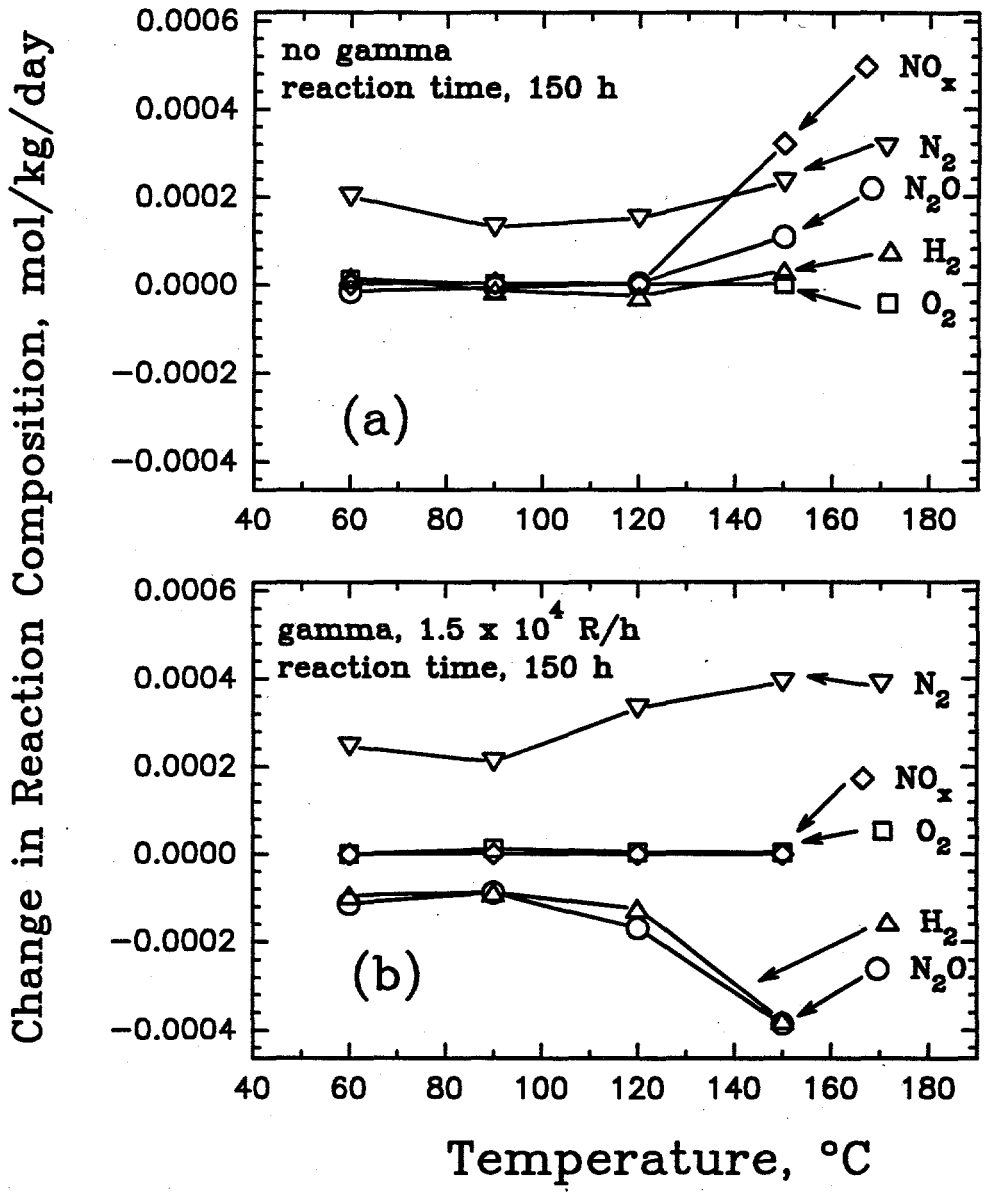

Figure 3.9. Gas Phase Composition of Hydrogen and Nitrous Oxide in Contact with Wet SY1-SIM-92A Centrifuged Solids at Termination of Reaction at Various Temperatures

In earlier work, radiolytic yields and reactant consumption for the gas phase reactions of hydrogen and nitrous oxide showed a strong dependence on total radiation dose and temperature (Bryan and Pederson 1995). G-values from this earlier work are given in Table 3.10 for the gas phase reaction of nitrous oxide with hydrogen and for nitrogen, oxygen, and ammonia formation. These values are also displayed in Figure 3.10. The smallest (absolute) values for $G(N_2O)$ and $G(H_2)$ were obtained at 60°C and grow increasingly more negative with increasing temperature. This behavior contrasts with results described in Section 3.1, where it was shown that the radiolytic decomposition of nitrous oxide to nitrogen and oxygen was essentially independent of temperature. The value of $G(N_2O)$ in the presence of hydrogen is approximately double that determined in its absence (see Tables 3.5 and 3.10). The observation that $G(N_2O)$ and $G(H_2)$ are essentially identical for each experiment indicates that an added pathway for nitrous oxide decomposition exists beyond the mechanisms discussed in Section 3.1.

The G-values for reactions of nitrous oxide with hydrogen in contact with dried and wet simulated waste are contained in Tables 3.11 an 3.12. These values are also depicted in Figures 3.11 and 3.12. As with the gas phase reactions of nitrous oxide and hydrogen discussed above, there is a large temperature dependence for the decomposition of nitrous oxide and hydrogen in contact with wet simulated waste. The effect of temperature was most significant at 150°C, where a large negative G-value for NO_x was also observed. At lower temperatures, $G(NO_x)$ was small and essentially negligible, but at 150°C the value decreases to approximately -20 molecules/100 eV. NO_x is not present in the gas phase at the beginning of the reaction, but it is present in the product of the thermal reaction at significant levels in the 150°C experiment containing wet simulated waste and absent from the companion radiolytic experiment. This observation is interpreted as a thermal production of NO_x followed by a radiolytic decomposition of this gas within this system.

In addition to increased consumption of nitrous oxide and hydrogen, ammonia yields also increased slightly with increased temperature in the gas phase experiments reported in Bryan and Pederson (1995). Ammonia yields are also included in Table 3.10. As more ammonia was produced, a concomitant decrease in molecular nitrogen production was observed. At 60°C, nitrogen yields nearly matched the nitrous oxide consumption. Nitrogen accounted for only one-third to one-half of the

Table 3.10. G-Value Measurements for the Gas Phase Reaction of Nitrous Oxide with Hydrogen

G-Value (molecule/100 eV)						
$G(N_2O)$	$G(H_2)$	$G(N_2)$	$G(O_2)$	$G(NH_3)$	Conditions	Dose (R)
-21.8	-15.7	19.3	2.06	0.35	60°C	7.2×10^6R
-36.2	-36.8	13.2	0.92	0.73	90°C	7.7×10^6R
-29.1	-29.1	13.6	0.14	0.76	120°C	7.4×10^6R
-38.0	-35.9	18.3	0.18	0.024	150°C	7.4×10^6R

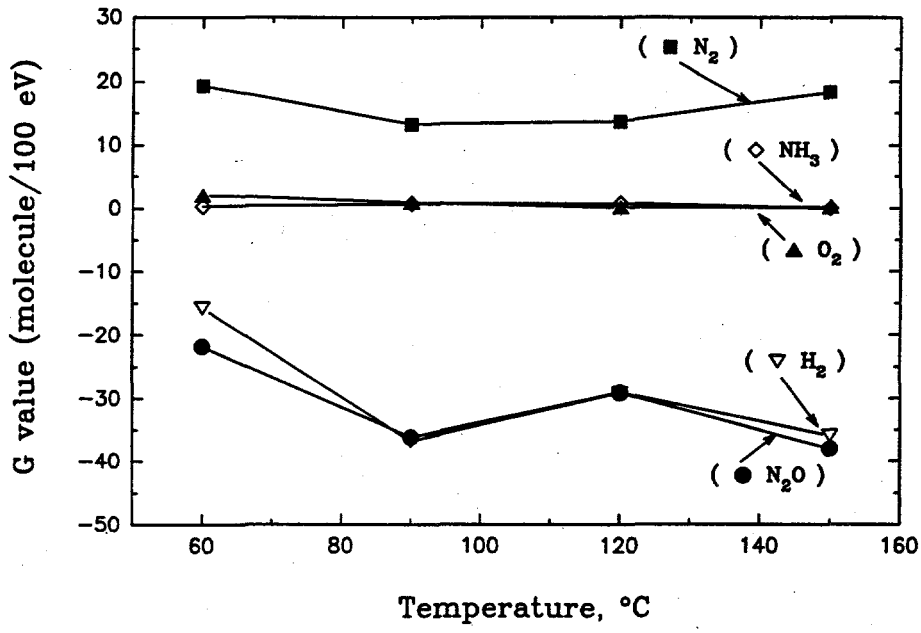

Figure 3.10. G-Values for the Gas Phase Reaction of Hydrogen with Nitrous Oxide

Table 3.11. G-Value Measurements for the Reaction of Nitrous Oxide and Hydrogen in Contact with Dried SY1-SIM-92A Simulated Waste

G-Value (molecule/100 eV)						
N_2O	N_2	O_2	H_2	NO_x	Dose (R)	Conditions
-5.52	8.46	0.57	-6.58	-0.106	4.65E+06	60°C; dried SY1-SIM-92A[a]
-1.50E-01	2.31E-01	1.56E-01	-1.80E-01	-2.88E-03	4.65E+06	60°C; dried SY1-SIM-92A[b]
-8.54	6.87	1.00	-5.54	-0.289	4.62E+06	90°C; dried SY1-SIM-92A[a]
-2.38E-01	1.91E-01	2.80E-2	-1.55E-1	-8.06E-3	4.65E+06	90°C; dried SY1-SIM-92A[b]
-6.77	9.75	0.995	-3.75	-0.415	4.64E+06	120°C; dried SY1-SIM-92A[a]
-2.04E-01	2.93E-01	3.00E-02	-1.13E-01	-1.25E-02	4.64E+06	120°C; dried SY1-SIM-92A[b]
-1.99	6.40	-0.243	-3.98	5.97	4.65E+06	150°C; dried SY1-SIM-92A[a]
-6.18E-02	1.99E-01	-7.55E-03	1.24E-01	1.85E-01	4.65E+06	150°C; dried SY1-SIM-92A[b]

(a) G-value calculation based on mass of gas phase only.
(b) G-value calculation based on total mass.

Table 3.12.. G-Value Measurements for the Reaction of Nitrous Oxide with Hydrogen in Contact with Centrifuged, Wet SY1-SIM-92A Simulated Waste

G-Value (molecule/100 eV)						
N_2O	N_2	O_2	H_2	NO_x	Dose (R)	Conditions
-9.6	4.57	-1.14	-10.96	-0.108	4.65E+06	60°C; wet SY1-SIM-92A; (a)
-2.63E-01	1.25E-01	-3.12E-02	-3.01E-01	-2.97E-03	4.65E+06	60°C; wet SY1-SIM-92A; (b)
-7.69	7.83	1.09	-7.11	-0.123	4.62E+06	90°C; wet SY1-SIM-92A; (a)
-2.18E-01	2.22E-01	3.09E-02	-2.02E-01	-3.48E-03	4.62E+06	90°C; wet SY1-SIM-92A; (b)
-13.63	14.49	0.362	-7.74	-0.165	5.01E+06	120°C; wet SY1-SIM-92A; (a)
-4.28E-01	4.56E-01	1.14E-02	-2.43E-01	-5.21E-03	5.01E+06	120°C; wet SY1-SIM-92A; (b)
-30.8	9.94	0.1767	-25.49	-19.98	4.65E+06	150°C; wet SY1-SIM-92A; (a)
-1.31E+0	4.23E-01	7.50E-03	-1.09E+0	-8.51E-01	4.65E+06	150°C; wet SY1-SIM-92A; (b)

(a) G-value calculation based on mass of gas phase only.
(b) G-value calculation based on total mass.

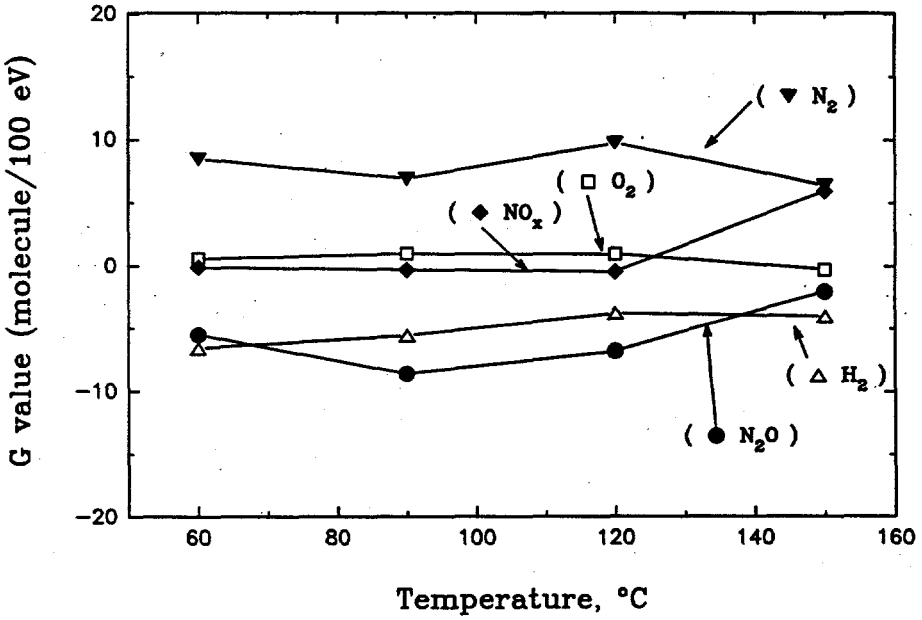

Figure 3.11. G-Value Measurements for Reaction of Hydrogen and Nitrous Oxide in Contact with Dried Centrifuged SY1-SIM-92A Solids

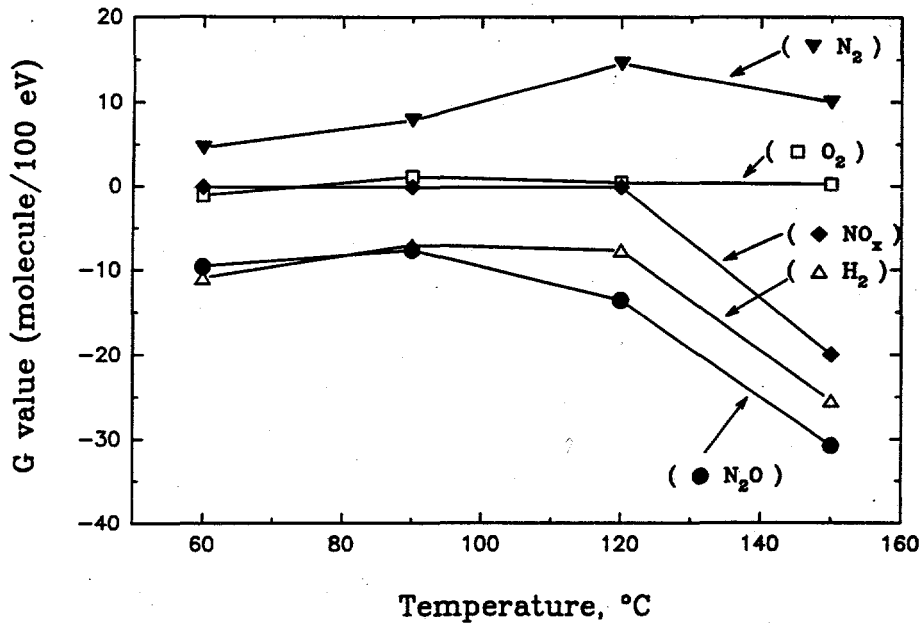

Figure 3.12. G-Value Measurements for Reaction of Hydrogen and Nitrous Oxide in Contact with Wet Centrifuged SY1-SIM-92A Solids

quantity of nitrous oxide consumed at 90 and 120°C, however. This coincides with increased ammonia production. In contrast to the work reported for the gas phase reactions of nitrous oxide and hydrogen (Bryan and Pederson 1995), when these gases are in contact with simulated waste, no measurable amount of ammonia is produced (Tables 3.8 and 3.9), most likely due to the immediate reaction of ammonia with the nitrate and nitrite oxidants present in the waste simulant.

3.3.2 Thermally Driven Reactions of Nitrous Oxide and Hydrogen: Literature Review and Discussion

Compared with other oxides of nitrogen, nitrous oxide is considered to be relatively unreactive (Samsonov 1973; Jones 1975; Cotton and Wilkinson 1980). Nitrous oxide will react with hydrogen following

$$N_2O + H_2 \rightarrow N_2 + H_2O \qquad (26)$$

Hydrogen/nitrous oxide reactions are more exothermic than analogous reactions of hydrogen in air or oxygen because nitrous oxide has a higher free energy (and heat) of formation than molecular oxygen. Autoignition temperatures are also lower for nitrous oxide/hydrogen mixtures than for corresponding mixtures of hydrogen with oxygen or air. Explosion limits for nitrous oxide and hydrogen mixtures are extremely wide (Jones 1975). The apparent downward lean limit is 6% for hydrogen in nitrous oxide for spark ignition compared with 8% for H_2 in air (Hertzberg and Zlochower 1994). The true

limit appears to be much lower. Using a pyrotechnic initiator of 1000 J, the apparent limit is approximately 2% hydrogen in nitrous oxide. Even smaller values were reported using more energetic pyrotechnic initiators (Hertzberg and Zlochower 1994). Nitrous oxide and hydrogen mixtures diluted with up to 79% nitrogen may still be explosive (Jones 1975).

Rates of reaction of hydrogen and nitrous oxide are not dependent simply on the rate of dissociation of nitrous oxide but on the concentrations of both nitrous oxide and hydrogen. Melville (1934) suggested the following scheme:

$2\ N_2O \rightarrow N_2O^* + N_2O$	(initiation)	(27)
$N_2O + H_2 \rightarrow N_2O^* + H_2$	(initiation)	(28)
$N_2O \rightarrow N_2 + O$	(initiation)	(29)
$O + H_2 \rightarrow OH + H$	(initiation)	(30)
$H + N_2O \rightarrow OH + N_2$	(propagation)	(31)
$OH + H_2 \rightarrow H_2O + H$	(propagation)	(32)
$H + H \rightarrow H_2$	(termination)	(33)

The symbol * in the reactions above indicates a molecule activated through collisions.

Nitrous oxide and hydrogen reactions may be catalyzed by solid surfaces. Reaction following Equation (26) on gold surfaces is of a very unusual type (Hutchinson and Hinshelwood 1926; Laidler 1965). This reaction is an example of noncompetitive adsorption, where the two molecules adsorb on different surface sites without displacing one another from the metal surface. Rates of reaction are very different from the more common case of a gas molecule interacting with an adsorbed molecule. No literature has been found describing nitrous oxide and hydrogen reactions catalyzed by materials other than gold. As described in Section 3.1.2, however, nitrous oxide reactions are most effectively catalyzed by p-type metal oxides, whereas hydrogen reactions are most effectively catalyzed by metals and n-type metal oxides (Laidler 1965). Preferential adsorption sites on a solid surface for the two gases are thus likely to be quite different in character.

Nitrous oxide consumption was greater in the presence of hydrogen than in its absence for the gas phase reactions (Bryan and Pederson 1995), consistent with earlier findings that nitrous oxide/hydrogen reaction rates depend on the concentration of both gases (Melville 1934; Laidler 1965). The consumption of nitrous oxide was always slightly greater than that of hydrogen, however, which is not expected if the overall reaction is described by Equation (26). From the work of Hertzberg and Zlochower (1994), it is apparent that even very small additions of hydrogen to nitrous oxide are effective in catalyzing decomposition reactions, which can occur explosively when initiated with a spark or pyrotechnic device. If hydrogen serves as a catalyst, it is not surprising that the stoichiometry of the reaction deviates from Equation (26).

In addition to the formation of water and nitrogen in the gas phase experiments following Equation (26), ammonia was also a product (Bryan and Pederson 1995). Ammonia formation under combined thermal and radiolytic conditions was more extensive than under thermal-only conditions, as described in Section 3.2.1. No literature was found that describes the direct conversion of nitrous oxide and hydrogen to ammonia under thermal or under combined thermal and radiolytic conditions. Nitrogen is a decomposition product of nitrous oxide, however, as described above. The reactions of nitrogen and hydrogen to yield ammonia are described in Section 3.3. No ammonia was found in the experiments

with simulated waste present; a plausible explanation for the lack of ammonia in systems containing simulated waste is that ammonia could be consumed by reaction with oxidants such as nitrite and nitrate within the simulated waste. It was shown previously that ammonia can react with nitrite or nitrate in the simulated waste tests described in Bryan and Pederson (1994).

Another potential product of the reaction of nitrous oxide and hydrogen is hydrazine (N_2H_4). Used as a rocket fuel, hydrazine will burn in air accompanied by considerable heat (149 kcal/mole) (Cotton and Wilkinson 1980). Hydrazine is also considered to be quite toxic (Sax 1979). In basic solutions, hydrazine is a strong reducing agent. Reactions that are known to produce hydrazine and involve nitrous oxide, hydrogen, or the reaction products nitrogen, oxygen, and/or ammonia are

$$N_2O + 3\ H_2 \rightarrow N_2H_4 + H_2O \quad (34)$$

$$N_2O + 2\ NH_3 \rightarrow N_2H_4 + H_2O + N_2 \quad (35)$$

$$2\ NH_3 + 1/2\ O_2 \rightarrow N_2H_4 + H_2O \quad (36)$$

Reactions (34) through (36) are considered to be of minor importance (Cotton and Wilkinson 1980). Rather, Reactions (37) through (39) are thermodynamically favored due to the strength of the N≡N bond:

$$N_2O + H_2 \rightarrow N_2 + H_2 \quad (37)$$

$$3\ N_2O + 2\ NH_3 \rightarrow 4\ N_2 + 3\ H_2O \quad (38)$$

$$2\ NH_3 + 3/2\ O_2 \rightarrow N_2 + 3\ H_2O \quad (39)$$

No hydrazine was observed by in these studies by mass spectrometry or in earlier tests by infrared spectroscopy (Bryan and Pederson 1995), under either thermal-only or combined thermal and radiolytic conditions, with or without simulated wastes. Hydrazine is highly soluble in water; any residual water that might be present could scavenge this compound. The boiling point of hydrazine is 113°C. All gas phase measurements were taken while the reaction vessels were maintained at temperature, so if any hydrazine product was formed, it would most likely have been observed, especially at the higher reaction temperatures of 90 to 150°C.

3.3.3 Combined Thermal and Radiolytic Reactions of Nitrous Oxide and Hydrogen

The addition of hydrogen to nitrous oxide has been reported to have little impact on the extent of radiolytic decomposition of nitrous oxide or on the formation of nitrogen (Hearne and Hummel 1961). Yields of oxygen and nitrogen oxides are reported to be less with hydrogen present, however (Hearne and Hummel 1961). After absorbing energy from impinging radiation, excited nitrous oxide molecules can decompose following (Anderson 1968):

$$N_2O^* \rightarrow N_2 + O \quad (40)$$

$$N_2O^* \rightarrow NO + N \quad (41)$$

Further reactions of the O and N atoms with nitrous oxide can occur:

$$N + N_2O \rightarrow N_2 + NO \quad (42)$$

$$O + N_2O \rightarrow N_2 + O_2 \quad (43)$$

$$O + N_2O \rightarrow 2\ NO \quad (44)$$

Hydrogen molecules can react with atomic oxygen:

$$H_2 + O \rightarrow OH + H \quad (45)$$

which would suppress both Reactions (43) and (44), thereby lowering both oxygen and nitric oxide yields. Hydrogen atoms may also react with nitrous oxide molecules to form molecular nitrogen and hydroxyl radicals (Hearne and Hummel 1961):

$$H + N_2O \rightarrow N_2 + OH \quad (46)$$

In the previous study, the quantities of nitrous oxide consumed in combined radiolytic and thermal reactions were substantially increased by the presence of hydrogen (Bryan and Pederson 1995). As given in Table 3.10 for gas phase reactions, the value of $G(N_2O)$ in the presence of hydrogen was more than double that without hydrogen in the reaction mixture (see Table 3.5). The rate-determining step in the thermal and radiolytic reaction of hydrogen and nitrous oxide cannot simply be the unimolecular decomposition of nitrous oxide; processes such as Reaction (46) must also be important.

In the present study, the amount of nitrous oxide consumed in combined radiolytic and thermal reactions was not appreciably increased by the presence of hydrogen when simulated waste was added to the system. For both the wet and dried centrifuged solids in contact with mixtures of nitrous oxide and hydrogen, the G-values for decomposition are similar to that of nitrous oxide alone with simulated waste present. This is in contrast to the observed trends for G-values measured for the gas phase reactions alone. Bryan and Pederson (1995) reported G-values for the decomposition of nitrous oxide and hydrogen ranging from about -15 to -40 molecules per 100 eV (for both $G(N_2O)$ and $G(H_2)$ over the temperature range of 60 to 150°C when both gases were present; the G-values measured for the decomposition of N_2O as the lone gas-phase component was invariant and approximately -12 molecules per 100 eV over the entire temperature range of 25 to 150°C. The smaller G-values (compared with those for gas phase reaction of N_2O and H_2O) resulting from the addition of hydrogen to nitrous oxide in the presence of simulated waste is due to the thermal activity of these gases in the presence of the added solids.

The extent of consumption of nitrous oxide in Tank 241-SY-101 via reaction with hydrogen in the gas phase was estimated by Bryan and Pederson (1995). Assuming a dose rate of 1000 R/h, a gas composed of approximately 30 mole percent nitrogen, 30 mole percent nitrous oxide, 30 mole percent hydrogen, and 10 percent ammonia, a value of $G(N_2O)$ of -30 molecules/100 eV, and assuming that all the absorbed energy is channeled into nitrous oxide/hydrogen reactions, approximately 2.2% of the nitrous oxide will be consumed per year. Although greater than the quantity consumed by the

unimolecular decomposition of nitrous oxide (0.9%), reactions of nitrous oxide and hydrogen by combined radiolytic and thermal reactions would still not appear to be high enough to measurably alter gas product distributions in the Hanford Site waste tanks.

The extent of radiolytic reaction was not enhanced via catalysis by tank solids for reactions containing N_2O and H_2. This was evidenced by the G-values for the systems with solids present being approximately equal to or less than those for the systems without solids (gas phase only).

3.4 Reactions of Nitrogen and Hydrogen

Nitrogen and hydrogen are two of the principal gases produced by thermal and radiolytic reactions in Tank 241-SY-101, each accounting for approximately 30 mole percent of the total (LANL 1994). Nitrogen and hydrogen are known to react to produce ammonia under thermal and radiolytic conditions. Experimental results on thermal and on combined thermal and radiolytic reactions of nitrogen and hydrogen in the presence of simulated waste are described in Section 3.4.1. In Section 3.4.2, thermally driven reactions of nitrogen and hydrogen are discussed. Section 3.4.3 addresses nitrogen and hydrogen reactions under combined thermal and radiolytic conditions.

3.4.1 Experimental Results for Reactions of Nitrogen and Hydrogen

Reactions of nitrogen and hydrogen were assessed under both thermal-only and combined thermal and radiolytic conditions in the presence of simulated Tank 241-SY-101 waste. Reactions were performed in stainless steel vessels with a capacity of $\approx$50 mL. Reaction times extended to approximately 150 hours, the reaction temperatures were 60, 90, 120, and 150°C, and radiation dose rates were 0 and 1.7×10^6 R/h. The concentration of the initial gas phase of each reaction was 94.98% N_2 and 5.02% H_2. This gas mixture was injected into each reaction vessel initially purged with argon and containing 5 g of simulated waste. Gas analyses were performed after the experiment by mass spectrometry and infrared spectroscopy. Data for the reaction of nitrogen with hydrogen in contact with simulated waste solids is presented in Tables 3.13 and 3.14 and Figures 3.13 and 3.14 for the dried and wet solids, respectively.

Hydrogen was consumed in the radiolytic reactions containing dry and wet simulated waste, as shown in Figures 3.13 and 3.14, respectively. The consumption of hydrogen in the thermal experiments was not as prevalent as in the radiolytic experiments. The radiolytic hydrogen consumption was greater for the gas in contact with the dried simulant waste (Figure 3.13b) than for the wet simulated waste reaction (Figure 3.14b). Hydrogen production for the radiolysis of water in the wet simulated waste system is believed to compensate for the reduced rate of hydrogen consumption in this system.

The production of nitrogen is evident in most all the reactions of dried and wet simulated waste under thermal and thermal-radiolytic conditions. Even with nitrogen added initially as a reactant gas in this system, nitrogen was shown to be produced by the decomposition of nitrate and nitrite in this system (Section 3.1). The reaction of nitrite and nitrate with reductants such as organics, under radiolytic and thermal conditions leading to the formation of reduced products such as nitrogen, nitrous oxide, and ammonia has been established (Bryan and Pederson 1994, 1995). The reaction of nitrate and nitrite with hydrogen has been shown to lead to the same products (Pederson and Bryan 1994).

Table 3.13. Gas Phase Compositions of Nitrogen and Hydrogen Reactions Under Thermal and Radiolytic Conditions (mixture contained dried SY1-SIM-92A simulated waste)

Gas Compositions, mol %							
N_2	H_2	N_2O	O_2	NO_x	NH_3	Dose (R)	Conditions
94.6	4.76	0.045	0.252	0	0	0	60°C, dried SY1-SIM-92A
96.7	2.69	0.322	0.081	0.007	0.006	2.31E+08	60°C, dried SY1-SIM-92A
94.93	4.65	0.061	0.279	0	0	0	90°C, dried SY1-SIM-92A
96.88	2.85	0.105	0.092	0	0	2.39E+08	90°C, dried SY1-SIM-92A
95.1	4.56	0.022	0.229	0	0	0	120°C, dried SY1-SIM-92A
96.39	3.15	0.235	0.161	0	0	2.36E+08	120°C, dried SY1-SIM-92A
95.1	4.46	0.094	0.254	0.045	0	0	150°C, dried SY1-SIM-92A
94.2	4.28	0.99	0.181	0.266	0	2.33E+08	150°C, dried SY1-SIM-92A

Table 3.14. Gas Phase Compositions of Reaction of Nitrogen and Hydrogen Under Thermal and Radiolytic Conditions (mixture contained centrifuged wet SY1-SIM-92A simulated waste)

Gas Compositions, mol %							
N_2	H_2	N_2O	O_2	NO_x	NH_3	Dose (R)	Conditions
94.6	4.71	0.046	0.24	0	0.003	0	60°C; wet SY1-SIM-92A
96.5	3.2	0.044	0.048	0	0	2.36E+08	60°C; wet SY1-SIM-92A
94.9	4.76	0.043	0.171	0.011	0	0	90°C; wet SY1-SIM-92A
96.7	3.04	0.035	0.127	0	0	2.34E+08	90°C; wet SY1-SIM-92A
91.4	4.67	2.38	0.003	1.53	0	0	120°C; wet SY1-SIM-92A
96.9	2.94	0.031	0.116	0.002	0	2.38E+08	120°C; wet SY1-SIM-92A
78.2	3.9	16.9	0.019	0.97	0	0	150°C; wet SY1-SIM-92A
95.2	4.32	0.38	0.063	0.014	0	2.33E+08	150°C; wet SY1-SIM-92A

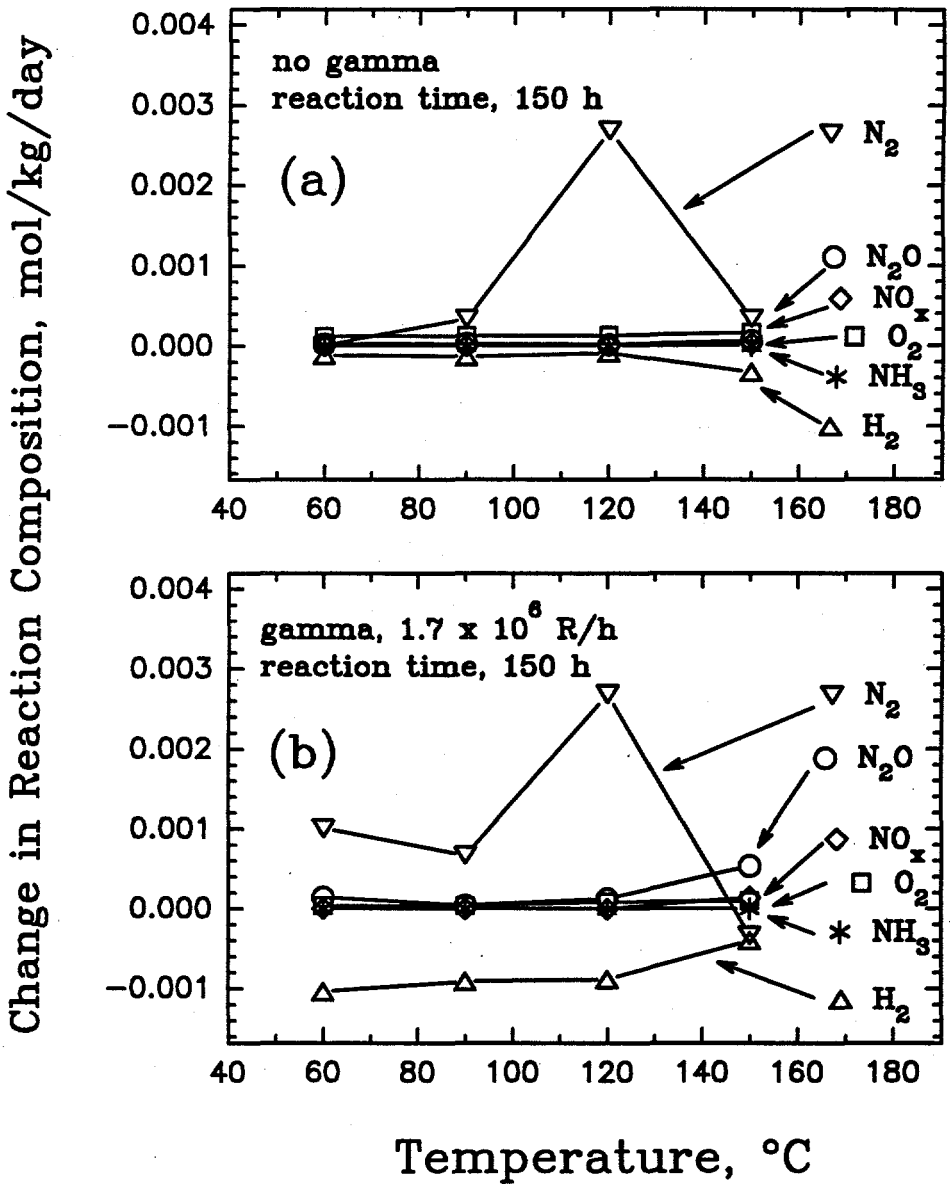

Figure 3.13. Gas Phase Composition of Hydrogen and Nitrogen in Contact with Dried SY1-SIM-92A Centrifuged Solids at Termination of Reaction at Various Temperatures

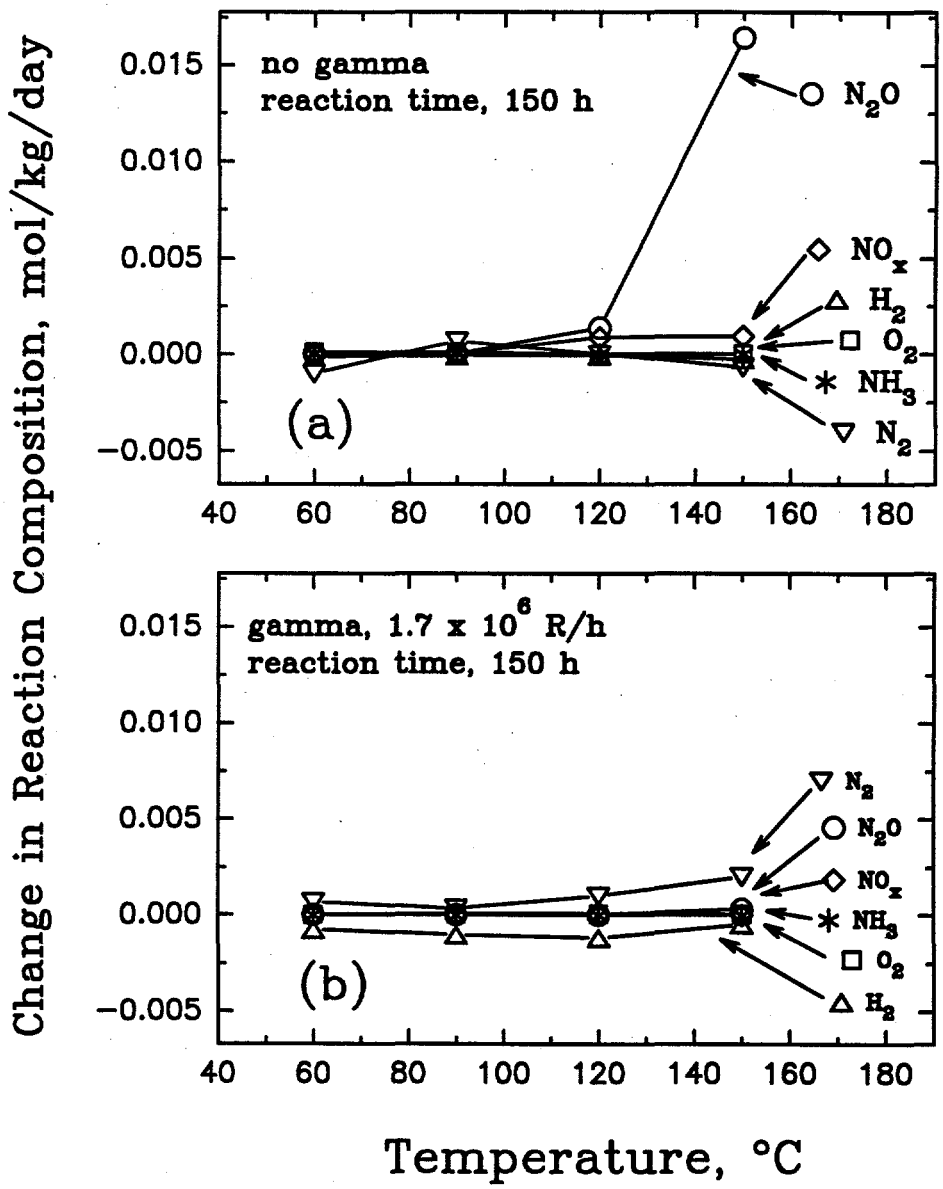

Figure 3.14. Gas Phase Composition of Hydrogen and Nitrogen in Contact with Wet SY1-SIM-92A Centrifuged Solids at Termination of Reaction at Various Temperatures

In the earlier studies using gas phase reactants alone, ammonia was formed from the reaction of nitrogen and hydrogen under both thermal-only and combined thermal and radiolytic conditions (Bryan and Pederson 1995). Thermal yields were found to be near the detection limit by infrared spectrometry. Ammonia yields increased with increased total radiation dose. It was not possible to assess any dose rate dependence from these tests. An inverse relation between total dose and $G(NH_3)$ was found in this earlier study. Values for $G(NH_3)$ are given in Table 3.15 and Figure 3.15 as a function of total radiation dose. Radiolytic ammonia yields fell from a high of nearly one molecule per 100 eV absorbed radiation for a total dose of 5.9×10^4 R/h to a low of approximately 0.01 molecules per 100 eV for a total dose of 1.1×10^7 R/h. This behavior may be ascribed to competing ammonia formation and decomposition reactions, leading to essentially a steady-state ammonia concentration. Values of $G(NH_3)$ corresponding to the lowest radiation doses are thus expected to be most reliable. The radiolytic decomposition of ammonia is treated in more detail in Section 3.5.

The G-values for the reaction of nitrogen and hydrogen in the presence of dried and wet simulated waste is summarized in Tables 3.16 and 3.17, respectively. This data is also shown in the respective Figures 3.16 and 3.17. In the wet simulated waste system, $G(N_2)$ is larger than this G-value for the system containing only SY1-SIM-92A simulated waste (Section 3.1). $G(H_2)$ is also negative in this system, although it was positive for this reaction in the simulated waste system in Section 3.1 that initially did not contain reactive gases. The increased radiolytic formation of nitrogen in this system compared with the system containing only simulated waste is due to the presence of hydrogen. Hydrogen, acting as a reductant toward nitrates and nitrites, has been shown to yield nitrogen, nitrous oxide, and ammonia, while consuming hydrogen.

Nitrous oxide is not initially present in the gas mixture containing nitrogen and hydrogen in contact with the dried or wet simulated waste in the reaction shown in Tables 3.16 and 3.17 and Figures 3.16 and 3.17. There is, however, a large negative G-value for nitrous oxide associated with the wet simulated waste system. The negative $G(N_2O)$ observed for the wet SY1-SIM-92A simulated waste system detailed in Figure 3.17 is interpreted as the thermal production of the nitrous oxide followed by the radiolytic decomposition of this compound. This interpretation is consistent with the observed production of nitrous oxide in the thermal reaction and the deficiency of nitrous oxide production in the radiolytic reaction.

There is a correlation with the radiolytic production of nitrogen and consumption of hydrogen in the dried simulated waste system. While $G(N_2)$ decreases with increasing temperature from 60 to 150°C, $G(H_2)$ increases over this same range. The decrease in radiolytic nitrogen production appears to be coupled with the radiolytic consumption of hydrogen. The action of hydrogen toward nitrates and nitrites has been established with the formation of reduced products including nitrogen, nitrous oxide, NO_x, and ammonia.

The lack of significant quantities of ammonia in either the wet or dried SY1-SIM-92A systems is counter to our observations when only the gas phase nitrogen and hydrogen were present. There is little doubt that this product should form under nearly identical conditions with the exception of added SY1-SIM-92A simulated waste being present. The absence of ammonia in the systems with waste present is most likely attributed to the reaction of the oxidants nitrite and nitrate with ammonia forming nitrogen, nitrous oxide, and other oxides of nitrogen, which effectively removes ammonia as it is being formed.

Table 3.15. G-Value Measurements for Gas Phase Reaction of Nitrogen and Hydrogen

G-Value (molecules/100 eV) $G(NH_3)$	Conditions	Dose
0.0099	90°C	1.1×10^7R
0.15	90°C	6.8×10^6R
0.25	90°C	4.2×10^5R
0.45	90°C	2.5×10^5R
0.74	90°C	9.6×10^4R
0.89	90°C	5.9×10^4R

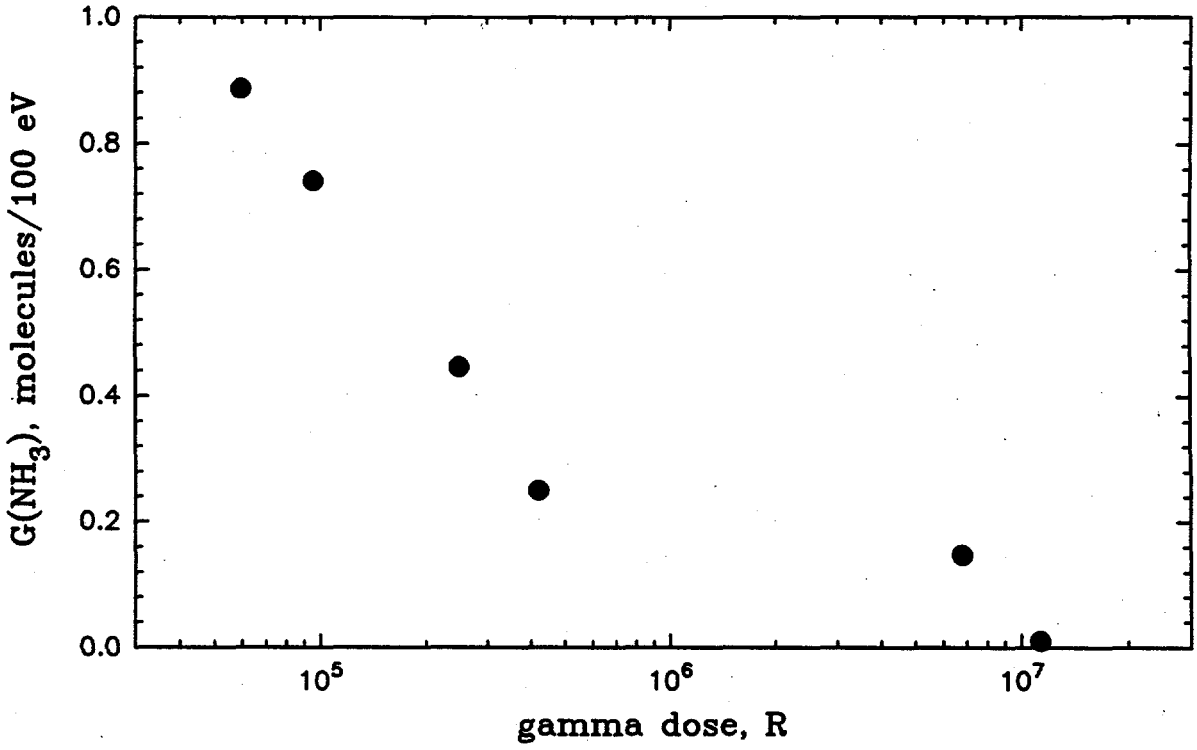

Figure 3.15. G-Values For Ammonia Production from Nitrogen and Hydrogen

Table 3.16. G-Value Measurements for Reaction of Nitrogen and Hydrogen in Contact with Dried SY1-SIM-92A Simulated Waste

G-Value (molecule/100 eV)							
N_2	H_2	N_2O	O_2	NO_x	NH_3	Dose (R)	Conditions
3.66	-3.36	0.449	-0.275	0.0114	0.00974	2.31E+08	60°C; dry SY1-SIM-92A[a]
2.59E-02	-2.38E-02	3.18E-03	-1.94E-03	8.04E-05	6.89E-05	2.31E+08	60°C; dry SY1-SIM-92A[b]
1.25	-2.88	0.068	-0.291	0	0	2.39E+08	90°C; dry SY1-SIM-92A[a]
8.34E-03	-1.93E-02	4.56E-04	-1.94E-03	0.00E+0	0.00E+0	2.39E+08	90°C; dry SY1-SIM-92A[b]
0	-2.48	0.351	-0.113	0	0	2.36E+08	120°C; dry SY1-SIM-92A[a]
0.00E+0	-2.00E-02	2.84E-03	-9.13E-04	0.00E+0	0.00E+0	2.36E+08	120°C; dry SY1-SIM-92A[b]
-1.74	-0.174	1.23	-0.156	0.301	0	2.33E+08	150°C; dry SY1-SIM-92A[a]
-1.50E-02	-1.49E-03	1.06E-02	-1.34E-03	2.58E-03	0.00E+0	2.33E+08	150°C; dry SY1-SIM-92A[b]

(a) G-value calculation based on mass of gas phase only.
(b) G-value calculation based on total mass.

Table 3.17. G-Value Measurements for the Reaction of Nitrogen with Hydrogen in Contact with Centrifuged, Wet SY1-SIM-92A Simulated Waste

G-Value (molecule/100 eV)							
N_2	H_2	N_2O	O_2	NO_x	NH_3	Dose (R)	Conditions
6.43	-2.23	-0.0055	-0.316	0	-0.0049	2.36E+08	60°C; wet SY1-SIM-92A; (a)
4.22E-02	-1.46E-02	3.64E-05	-2.08E-03	0.00E+0	-3.22E-05	2.36E+08	60°C; wet SY1-SIM-92A; (b)
-1.06	-2.91	-0.0153	-0.08055	-0.01812	0	2.34E+08	90°C; wet SY1-SIM-92A; (a)
-8.52E-03	-2.34E-02	-1.24E-04	-6.47E-04	-1.46E-04	0.00E+0	2.34E+08	90°C; wet SY1-SIM-92A; (b)
2.785	-3.04	-3.73	0.1772	-2.429	0	2.38E+08	120°C; wet SY1-SIM-92A; (a)
2.52E-02	-2.70E-02	-3.37E-02	1.60E-03	-2.20E-02	0.00E+0	2.38E+08	120°C; wet SY1-SIM-92A; (b)
5.36	-0.402	-32.21	0.066	-1.86	0	2.33E+08	150°C; wet SY1-SIM-92A; (a)
6.87E-02	-5.13E-03	-4.11E-01	8.45E-04	-2.37E-02	0.00E+0	2.33E+08	150°C; wet SY1-SIM-92A; (b)

(a) G-value calculation based on mass of gas phase only.
(b) G-value calculation based on total mass of system.

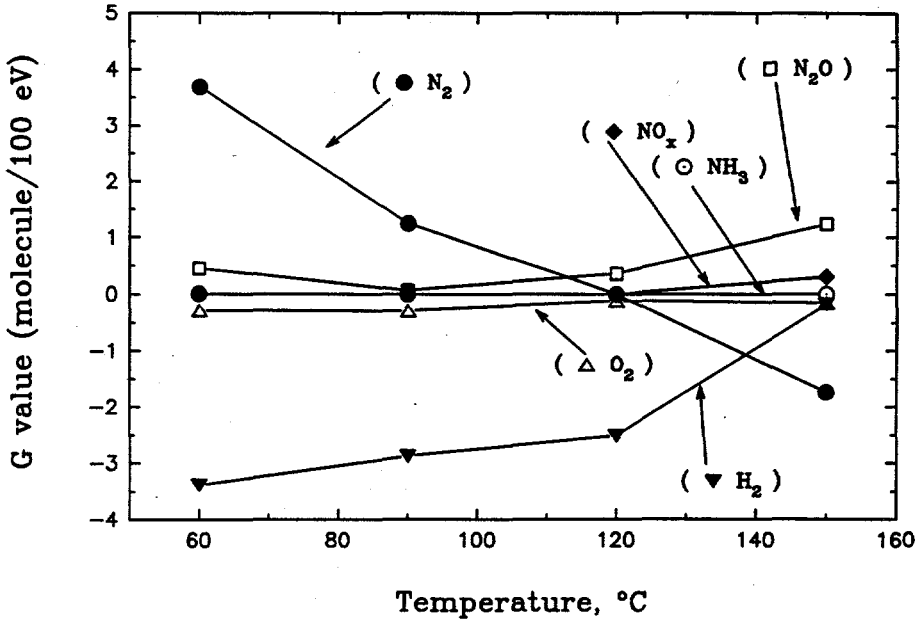

Figure 3.16. G-Value Measurements for Reaction of Hydrogen and Nitrogen in Contact with Dried, Centrifuged SY1-SIM-92A Solids

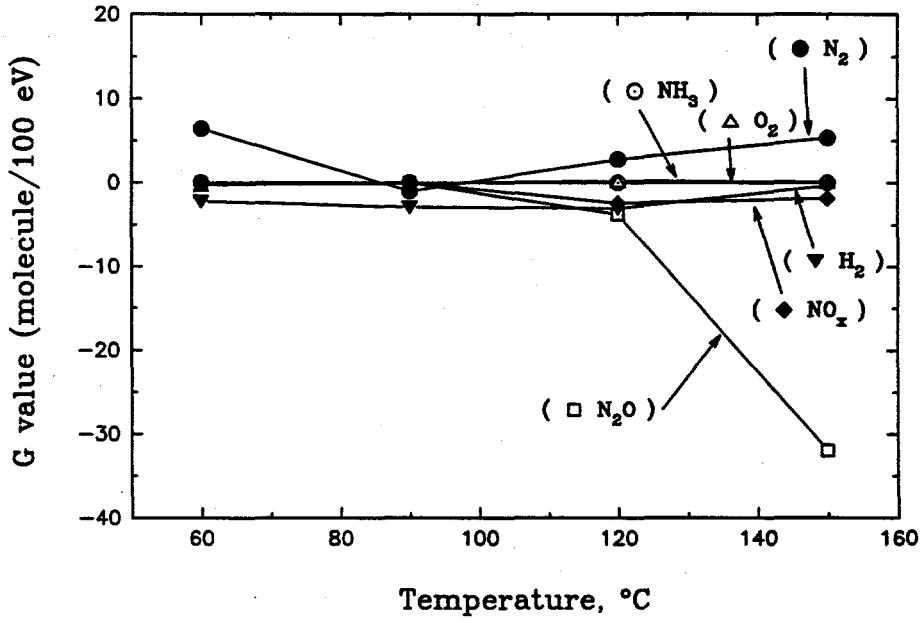

Figure 3.17. G-Value Measurements for Reaction of Hydrogen and Nitrogen in Contact with Wet Centrifuged SY1-SIM-92A Solids

3.4.2 Thermally Driven Reactions of Nitrogen and Hydrogen

The Haber process is used on an industrial scale to produce ammonia from the reaction of hydrogen and nitrogen in the presence of a catalyst (Thomas and Thomas 1969; Bottomley and Burns 1979). The reaction

$$N_2 + 3\,H_2 \rightarrow 2\,NH_3 \qquad (47)$$

is exothermic and is thermodynamically favored by low temperatures and high pressures. However, because of kinetic considerations, industrial ammonia synthesis is typically performed in the temperature range 400 to 550°C and 100 to 1000 atmospheres total pressure.

The use of catalysts in ammonia synthesis following Reaction (47) is essential (Thomas and Thomas 1969; Bottomley and Burns 1979; Cotton and Wilkinson 1980). Industrial catalysts commonly consist of reduced oxides of iron promoted with metal oxides such as alumina, silica, or zirconia. Alkali and alkaline earth promoters have also been used. The rate-determining step in ammonia synthesis from nitrogen and hydrogen is the dissociative adsorption of nitrogen onto those catalyst surfaces. In the absence of an appropriate catalyst and at temperatures relevant to Hanford Site waste tanks, the expected rate of ammonia formation from the thermally driven reaction of nitrogen and hydrogen is infinitesimally small. The observation of a small yield of ammonia in the gas phase experiments performed at 90°C without radiation almost certainly can be attributed to catalysis by the stainless steel reaction vessel.

3.4.3 Combined Radiolytic and Thermal Reactions of Nitrogen and Hydrogen

The synthesis of ammonia from its elements and the decomposition of ammonia by radiolytic processes has been studied extensively (Spinks and Woods 1990). Ammonia can be produced from the gas-phase reaction of hydrogen and nitrogen in the presence of gamma radiation. Ammonia yields are usually quite low, with $G(NH_3)$ ranging from $\approx$0.7 to 1.5 molecules/100 eV (Spinks and Woods 1990). For a gas mixture containing 30% nitrogen and 70% hydrogen at a total pressure of approximately 50 atm and at 25°C, $G(NH_3)$ has been given as 0.98 molecules/100 eV (CRC 1986). Results for $G(NH_3)$ corresponding to low total doses in this study are in good agreement with literature values.

The rapidly falling radiolytic yield of ammonia with increased dose shown in Figure 3.15 emphasizes that ammonia can not only be synthesized by radiolytic processes but also decomposed. Ammonia decomposition reactions are discussed in more detail in Section 3.5. A number of reaction pathways yield ammonia, both thermal and radiolytic, in the Hanford Site tank wastes. These have been addressed by Ashby et al. (1994b) and Meisel et al. (1993). Gas phase reactions of nitrogen and hydrogen by thermal and combined thermal and radiolytic processes ranks as only a very minor source of ammonia compared with solution phase reactions involving the nitrite ion and organic waste components. Radiolytic gas phase reactions may serve to limit the maximum concentration of ammonia that is possible rather than contribute substantially to the quantity produced.

3.5 Ammonia Decomposition Reactions

Ammonia is one of the main gases produced from thermal and radiolytic processes in Hanford Tank 241-SY-101 (Ashby et al. 1992; Babad et al. 1991, 1992; LANL 1994). From studies using simulated wastes, the kinetics of formation and the stoichiometry of these gaseous products have been shown to be sensitive to the composition of the waste mixture (Delegard 1980; Jansky and Meissner, in Reynolds et al. 1991; Ashby et al. 1992, 1993, 1994a,b; Meisel et al. 1991, 1992, 1993; Bryan et al. 1992, 1993; Bryan and Pederson 1994). The gas phase production of ammonia from its elements has been shown to be dose-dependent, indicative of the instability of the ammonia compound to decomposition under radiolytic and thermal conditions (Bryan and Pederson 1995). Gas phase and surface catalyzed reactions may be important in determining the final proportion of ammonia that is produced in Hanford Site waste tanks. In Section 3.5.1, the results of measurements to assess the rates of ammonia decomposition in the presence of simulated waste as a function of radiation dose and temperature are described. Section 3.5.2 includes a literature review of thermal decomposition mechanisms, both gas-phase and surface-catalyzed reactions. Section 3.5.3 addresses the radiolytic mechanisms.

3.5.1 Experimental Results for the Reaction of Ammonia with Simulated Waste

Ammonia decomposition reactions in the presence of simulated waste were assessed under thermal and combined thermal and radiolytic conditions. Reactions were conducted in stainless steel vessels in the temperature range of 60 to 150°C and gamma radiation doses of 0 and 10^7 rad; reaction times extended to approximately 70 hours. The reaction vessels were initially filled with 10% ammonia (balance argon) at one atmosphere total pressure. Gas compositions were analyzed by mass spectrometry before and after the tests.

The decomposition of ammonia was apparent for the reaction systems containing dry and wet SY1-SIM-92 waste simulant, in both thermal only and under thermal and radiolytic conditions, over the temperature range 60 to 150°C. The data are shown in Tables 3.18 and 3.19 and Figures 3.18 and 3.19 for the decomposition of ammonia in the presence of dried and wet simulated waste, respectively.

The reaction of ammonia shows a definite trend of being consumed with increasing temperature for both the dried and wet simulated waste under thermal-only conditions (Figures 3.18a and 3.19a) and under radiolytic and thermal conditions (Figures 3.18b and 3.19b). Although definitely temperature-dependent, the decomposition is more prominently facilitated in the radiolytic experiments. The data are displayed as change of reactant or product per kilogram waste simulant per day (mol/kg/day) as a function of reaction temperature.

Nitrogen is the most abundant product of the thermal decomposition of ammonia (see Figures 3.18a and 3.19a). The thermal nitrogen production is much higher than can be accounted for by the thermolysis of the SY1-SIM-92A simulant in the absence of ammonia (Section 3.1). Hydrogen (H_2) is produced thermally, but only in a slight amount, nearly indistinguishable from what can be produced from the thermolysis of SY1-SIM-92A alone (Section 3.1). Thermal hydrogen yields are low for the thermolysis of ammonia in the presence of simulated waste because the final product containing hydrogen is most likely not H_2. Water is the most likely product between ammonia (the reductant) and nitrate and nitrite (the oxidants) and is not included in Tables 3.18 and 3.19 and Figures 3.18 and 3.19.

Table 3.18. Gas Phase Compositions of Reaction of Ammonia Under Thermal and Radiolytic Conditions (mixture contained dried SY1-SIM-92A simulated waste)

Gas Compositions, mol %								
NH_3	N_2O	N_2	O_2	H_2	NO_x	Ar	Dose (R)	Conditions
7.2	0.013	0.405	0.046	0.007	0.018	91.9	0	60°C; dry SY1-SIM-92A
5.8	0.022	0.81	0.012	0.34	0.023	92.7	5.15E+07	60°C; dry SY1-SIM-92A
7.8	0.03	0.88	0.015	0.01	0.016	90.8	0	90°C; dry SY1-SIM-92A
5.3	0.011	1.19	0.003	0.56	0.014	92.6	5.44E+07	90°C; dry SY1-SIM-92A
4.9	0.132	2.73	0.52	0.111	0.019	91.3	0	120°C; dry SY1-SIM-92A
5.6	0.017	1.35	0.0045	0.426	0.004	92.3	5.24E+07	120°C; dry SY1-SIM-92A
4.1	0.013	1.05	0.014	0.0029	0.027	94.5	0	150°C; dry SY1-SIM-92A
4.3	0.005	2.6	0	0.464	0.017	92.4	5.38E+07	150°C; dry SY1-SIM-92A

Table 3.19. Gas Phase Compositions of Reaction of Ammonia Under Thermal and Radiolytic Conditions (mixture contained centrifuged, wet SY1-SIM-92A simulated waste)

Gas Compositions, mol %								
NH_3	N_2O	N_2	O_2	H_2	NO_x	Ar	Dose (R)	Conditions
11.7	0.006	0.546	0.064	0.003	0.013	87.7	0	60°C; wet SY1-SIM-92A
8.9	0.015	1.68	0.004	0	0.012	89.4	5.15E+07	60°C; wet SY1-SIM-92A
11.2	0.011	1.08	0.006	0	0.012	87.7	0	90°C; wet SY1-SIM-92A
9.3	0.006	1.2	0.005	0.591	0.009	88.8	5.27E+07	90°C; wet SY1-SIM-92A
8.7	0.031	1.27	0.01	0.054	0.045	89.4	0	120°C; wet SY1-SIM-92A
5.74	0.0074	0.463	0	0.495	0.0037	93	5.24E+07	120°C; wet SY1-SIM-92A
8.1	0.063	0.84	0.007	0.009	0.16	90.4	0	150°C; wet SY1-SIM-92A
4.4	0.002	1.75	0	1.46	0.006	92.1	5.38E+07	150°C; wet SY1-SIM-92A

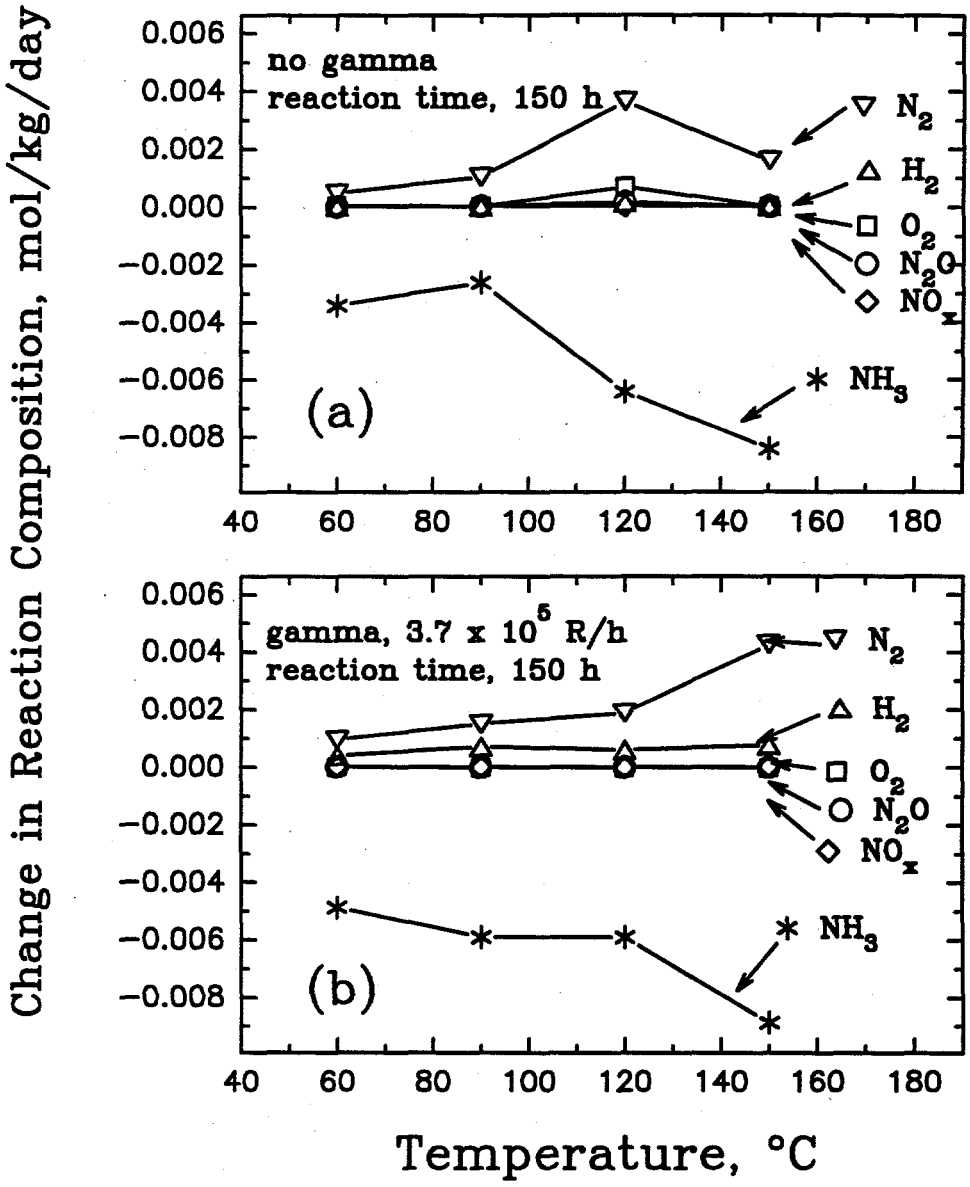

Figure 3.18. Gas Phase Composition of Ammonia in Contact with Dried SY1-SIM-92A Centrifuged Solids at Termination of Reaction at Various Temperatures

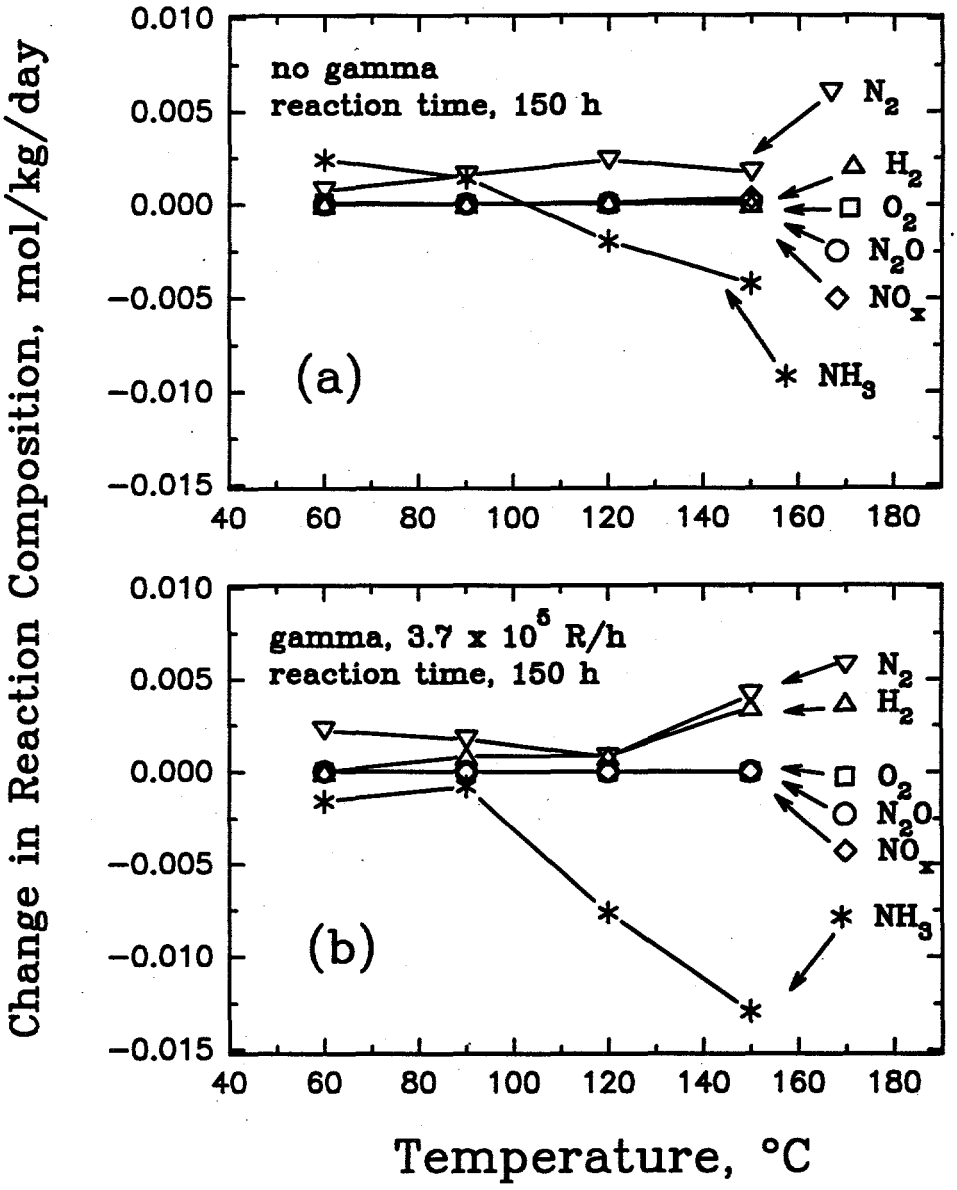

Figure 3.19. Gas Phase Composition of Ammonia in Contact with Wet SY1-SIM-92A Centrifuged Solids at Termination of Reaction at Various Temperatures

Nitrogen and hydrogen are the principal products of the radiolytic decomposition of ammonia in contact with the dried or wet simulated waste (Figures 3.18b and 3.19b, respectively). Hydrogen is produced in a greater fraction in the wet system than in the dried simulated waste system, most likely due to the co-production of that product by radiolysis of water.

The G-values for the decomposition of ammonia reactions in contact with SY1-SIM-92A simulated waste are included in Tables 3.20 and 3.21. These data are also shown in Figures 3.20 and 3.21. $G(NH_3)$ is negative for most all temperatures for both the dried and wet systems containing waste simulant. Several trends emerge for $G(NH_3)$ (see Figures 3.20 and 3.21): $G(NH_3)$ is generally more negative for the wet system than for the dried waste simulant system; this may be due to the higher availability of nitrate and nitrite in solution in the wet system compared with the dried system, allowing for the interaction of nitrite and nitrate with the soluble ammonia present in the reaction.

In the dried simulant system, $G(NH_3)$ is negative at low temperature but becomes more positive (essentially zero) at higher temperatures. This can be explained by observing the reactivity of ammonia in both the radiolytic and thermal experiments shown in Figure 3.19. There is a definite thermal component to the decomposition of ammonia in both the radiolytic and thermal only experiments. At high temperature the thermal component dominates, and the extent of ammonia decomposition is essentially equal for both thermal and radiolytic reactions.

The G-values for nitrogen and hydrogen production are much higher in the presence of ammonia than in the comparable experiment containing only SY1-SIM-92A (Section 3.1). This is explained by the direct decomposition of ammonia to yield nitrogen and hydrogen directly. The formation of nitrogen is also facilitated by the secondary reaction of ammonia with nitrate and nitrite to form nitrogen, nitrous oxide, other oxides of nitrogen, and water.

Small quantities of nitrous oxide and other oxides of nitrogen were produced thermally in the decomposition of ammonia in contact with wet and dried simulated waste. Even smaller quantities were observed in the radiolytic reactions. As a result, $G(N_2O)$ and $G(NO_x)$ are small and negative, in general, for both the wet and dried simulated waste in contact with ammonia.

3.5.2 Thermal Decomposition of Ammonia

As in the case of nitrous oxide decomposition reactions, ammonia decomposition via a homogeneous, unimolecular mechanism is important only at high temperatures. High temperatures are required because the NH_2-H bond dissociation energy is nearly 100 kcal/mole (Homann and Haas 1972). The heterogeneous decomposition catalyzed by solid surfaces is much more probable at temperatures relevant to Hanford Site tank wastes.

An expression for the rate constant for homogeneous ammonia decomposition has been given by Michel and Wagner (1965) for the temperature range of 2100K to 2900K:

$$k_{hom} = 4.4 \times 10^{12} \exp[-79.5\ (\pm 2.5)/RT]\ \text{l/mole-s} \qquad (48)$$

Table 3.20. G-Value Measurements for Reaction of Ammonia in Contact with Dried SY1-SIM-92A Simulated Waste

G-Value (molecule/100 eV)							
NH_3	N_2O	N_2	O_2	H_2	NO_x	Dose (R)	Conditions
-6.35	0.0463	2.08	-0.172	1.7	0.026	5.15E+07	60°C; dry SY1-SIM-92A[a]
-1.66E-01	1.21E-03	5.43E-02	-4.50E-03	4.43E-02	6.79E-04	5.15E+07	60°C; dry SY1-SIM-92A[b]
-12.52	-0.082	1.81	-0.0529	2.66	-0.0043	5.44E+07	90°C; dry SY1-SIM-92A[a]
-3.53E-01	-2.31E-03	5.10E-02	-1.49E-03	7.50E-02	-1.21E-04	5.44E+07	90°C; dry SY1-SIM-92A[b]
1.93	-0.556	-6.37	-2.51	1.64	-0.072	5.24E+07	120°C; dry SY1-SIM-92A[a]
5.92E-02	-1.70E-02	-1.95E-01	-7.69E-02	5.04E-02	-2.20E-03	5.24E+07	120°C; dry SY1-SIM-92A[b]
-1.41	-0.0352	8.15	-0.065	2.32	-0.0399	5.38E+07	150°C; dry SY1-SIM-92A[a]
-5.01E-02	-1.24E-03	2.89E-01	-2.31E-03	8.23E-02	-1.41E-03	5.38E+07	150°C; dry SY1-SIM-92A[b]

(a) G-value calculation based on mass of gas phase only.
(b) G-value calculation based on total mass of system.

Table 3.21. G-Value Measurements for Reaction of Ammonia in Contact with Centrifuged, Wet SY1-SIM-92A Simulated Waste

G-Value (molecule/100 eV)							
NH_3	N_2O	N_2	O_2	H_2	NO_x	Dose (R)	Conditions
-15.2	0.0448	5.66	-0.309	-0.015	-0.00619	5.15E+07	60°C; wet SY1-SIM-92A[a]
-4.44E-01	1.30E-03	1.65E-01	-9.00E-03	-4.51E-04	-1.80E-04	5.15E+07	60°C; wet SY1-SIM-92A[b]
-7.72	-0.0248	0.653	-0.00487	2.99	-0.0146	5.27E+07	90°C; wet SY1-SIM-92A[a]
-2.38E-01	-7.60E-04	2.02E-02	-1.50E-04	9.25E-02	-4.52E-04	5.27E+07	90°C; wet SY1-SIM-92A[b]
-16.33	-0.129	-4.51	-0.0533	2.132	-0.222	5.24E+07	120°C; wet SY1-SIM-92A[a]
-6.17E-01	-4.87E-03	-1.70E-01	-2.01E-03	8.05E-02	-8.38E-03	5.24E+07	120°C; wet SY1-SIM-92A[b]
-18.09	-0.256	5.11	-0.0295	7.21	-0.646	5.38E+07	150°C; wet SY1-SIM-92A[a]
-9.06E-01	-1.28E-02	2.56E-01	-1.48E-03	3.60E-01	-3.23E-02	5.38E+07	150°C; wet SY1-SIM-92A[b]

(a) G-value calculation based on mass of gas phase only.
(b) G-value calculation based on total mass of system.

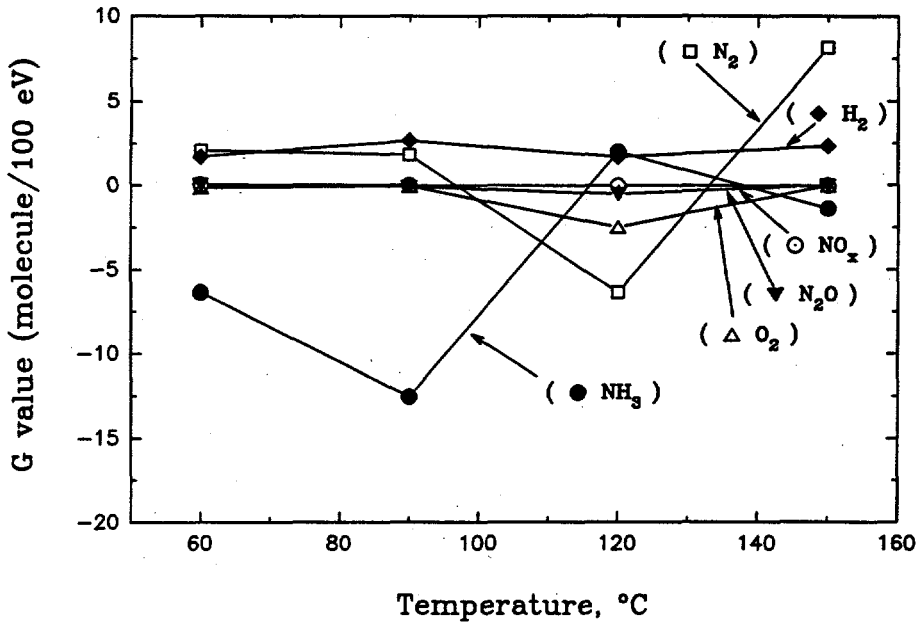

Figure 3.20. G-Value Measurements for Decomposition of Ammonia in Contact with Dried Centrifuged SY1-SIM-92A Solids

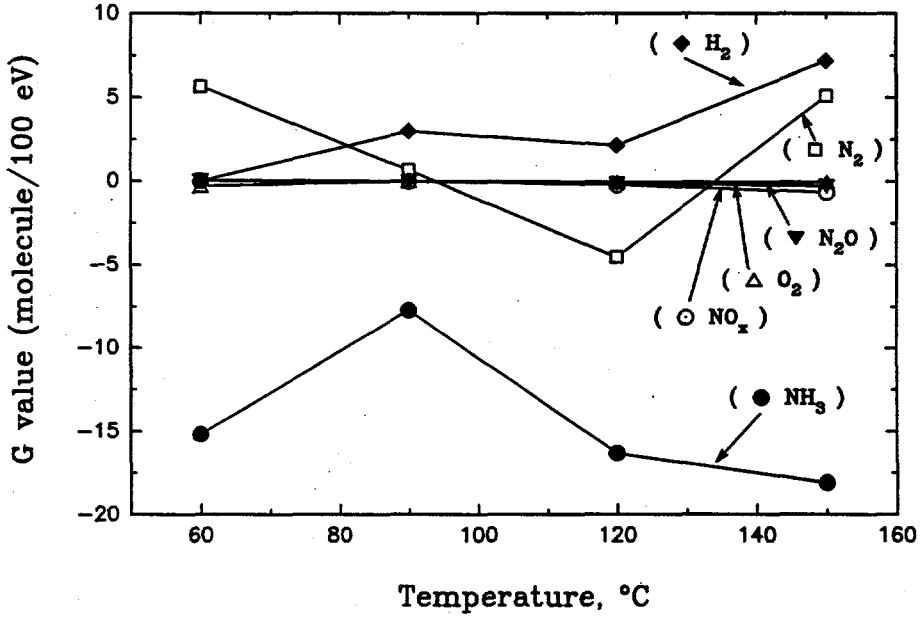

Figure 3.21. G-Value Measurements for Decomposition of Ammonia in Contact with Wet Centrifuged SY1-SIM-92A Solids

This second-order rate constant was first-order with respect to ammonia and the diluent argon. A similar expression has been given by Jacobs (1963) but with an activation energy of 77.7 kcal/mole and a pre-exponential factor of 2.5×10^{13} l/mole-s. Jacobs (1963) determined, based on shock tube experiments, that the reaction order with respect to ammonia was 3/2, while the order with respect to argon was 1/2. Regardless of which (if either) expression is correct, the extent of ammonia decomposition expected at tank temperatures by homogeneous unimolecular decomposition is infinitesimally small and can be neglected.

Substantially lower activation energies have been reported for ammonia decomposition reactions catalyzed by metal surfaces. Activation energies of 38 kcal/mole have been reported for tungsten surfaces (Hinshelwood and Burke 1925), 38 to 43 kcal/mole for molybdenum surfaces (Kunsman 1928) and 48 kcal/mole for osmium surfaces (Arnold and Burk 1932). From Equation (20), derived from absolute rate theory, and using a value of $\Delta E \approx 40$ kcal/mole, it is estimated that heterogeneous reactions should dominate for temperatures less than approximately 450°C. Of course, that estimate will change substantially, depending on the catalytic activity of the solid surface. The extent of decomposition of ammonia by either homogeneous or heterogeneous pathways at tank temperatures is expected to be extremely small, however (Homann and Haas 1972).

3.5.3 Radiolytic Decomposition of Ammonia

Ammonia is decomposed under radiolytic conditions. Depending on the temperature, dose rate, and ammonia partial pressure, products include nitrogen, hydrogen, and hydrazine. Radiolytic reactions involving ammonia have been reviewed by Spinks and Woods (1990), from which much of the following discussion has been taken.

Unlike nitrous oxide decomposition reactions under radiolytic conditions, which are largely temperature-independent at moderate temperatures, G-values for ammonia decomposition are temperature-dependent. The value for $G(-NH_3)$ increases from 0.35 μmol/J at 20°C to a plateau of approximately 1 μmole/J at 150°C for an ammonia partial pressure of 1 atm. The value for $G(-NH_3)$ also depends on the ammonia partial pressure, falling from a value of 0.40 μmol/J at 0.1 atm to 0.35 μmol/J at 1 atm at 20°C. At 120°C, $G(-NH_3)$ falls from 1 μmole/J at 1 atm to 0.68 μmole/J at 60 atm. These trends emphasize the finding that ammonia decomposition reactions are quite complex and involve multiple steps.

From $G(-NH_3)$ values obtained in the literature, the extent of radiolytic decomposition of ammonia in the gas phase in Hanford Site waste tanks can be estimated. As before, a gamma dose rate of 1000 R/h is assumed. A $G(-NH_3)$ value of 6.3 molecules/100 eV is estimated from the work of Sorokin and Pshezhetskii (1964), corresponding to a temperature of 60°C and an ammonia partial pressure of 0.2 atm. In one year, it is calculated that 0.15% of the ammonia initially present in the wastes will be decomposed to nitrogen and hydrogen. Such losses will be more than offset by the production of ammonia via complexant degradation reactions (Ashby et al. 1994b; Meisel et al. 1993; Bryan and Pederson 1994).

4.0 Summary and Conclusions

This report describes the results of tests to evaluate the rates of thermal and combined thermal and radiolytic reactions involving flammable gases in the presence of Tank 241-SY-101 simulated waste. Flammable gases generated by the radiolysis of water and by the thermal and radiolytic decomposition of organic waste constituents may themselves participate in further reactions. Examples include the decomposition of nitrous oxide to yield nitrogen and oxygen, the reaction of nitrous oxide and hydrogen to produce nitrogen and water, and the reaction of nitrogen and hydrogen to produce ammonia. The composition of the gases trapped in bubbles in the wastes might therefore change continuously as a function of the time that the gas bubbles are retained.

The reactivities of essentially pure nitrous oxide, nitrous oxide and hydrogen mixtures, and nitrogen and hydrogen mixtures were evaluated under thermal and combined thermal and radiolytic conditions. Tests were performed in stainless steel vessels in the temperature range of 60 to 150°C, with ^{60}Co gamma irradiation doses from 0 to more than 10^7 rad and reaction times extending to approximately 70 hours. The tests included Hanford Tank 241-SY-101 simulated waste and dried simulated waste solids.

The primary radiolytic/thermal products of nitrous oxide decomposition were nitrogen, oxygen, and nitrogen dioxide. Under thermal-only conditions, the extent of nitrous oxide decomposition was less than that for the companion experiment under combined thermal and radiolytic conditions. However, the thermal decomposition in the presence of simulated waste was significant compared with that observed in earlier tests performed in the absence of simulated waste (Bryan and Pederson 1995). G-values measured for the decomposition of nitrous oxide in the presence of simulated waste showed a significant temperature dependence consistent with a surface reaction with nitrous oxide contributing to the decomposition reaction. $G(N_2O)$ ranged in value from -7 to -17 molecules per 100 eV in the systems containing wet and dried simulated waste.

In contrast, $G(N_2O)$ for the gas phase decomposition of nitrous oxide was determined to be constant at -12 molecules/100 eV, in good agreement with literature values. No temperature dependence of $G(-N_2O)$ was apparent from 60 to 150°C. Nitrogen dioxide yields decreased with increasing temperature, while nitrogen yields increased with increasing temperature. Assuming a gamma dose rate of 1000 R/h in the actual wastes, and assuming that nitrous oxide composes $\approx 30\%$ of the gases trapped in the nonconvecting layer, it is estimated that $\approx 1\%$ of the retained nitrous oxide could be consumed by these gas phase radiolytic reactions per year. However, the thermal decomposition of nitrous oxide contributes significantly to the total decomposition of nitrous oxide when in contact with simulated waste.

Catalysis of nitrous oxide decomposition by solid phases present in the waste is a significant possibility. At least some of the gases will be retained as bubbles attached to solid particles, in response to surface tension forces. Thus the gases will be in intimate contact with tank solids, including sodium aluminate, sodium nitrate, sodium nitrite, sodium carbonate, and other phases. From results of this study, the catalysis of nitrous oxide decomposition by such solids is a possibility. The temperature dependence of the G-value for the decomposition of nitrous oxide in the presence of wet or dried waste simulant solids shows that a thermal component is involved. By contrast, the gas phase

reaction showed no thermal sensitivity over the same temperature range (Bryan and Pederson 1995). In addition, the thermal reaction of nitrous oxide in the presence of simulated waste solids showed significant conversion of nitrous oxide to other gas products, while under similar conditions, the gas phase reaction showed no conversion under thermal conditions alone. Based on data within this report, and assuming a pseudo-zero order, surface catalyzed reaction for the decomposition of nitrous oxide in contact with the waste, it can be estimated that from ≈ 20 to $\approx 90\%$ of the nitrous oxide could be decomposed in one year.

In earlier studies it was found that under thermal-only conditions the principal products of the gas phase reaction of nitrous oxide with hydrogen were nitrogen, oxygen, water, and a very small concentration of ammonia (Bryan and Pederson 1995). Under combined thermal and radiolytic conditions, while similar products were found, the extent of nitrous oxide and hydrogen consumption and of ammonia formation was considerably greater.

Similar trends are observed for the reaction of nitrous oxide with hydrogen in contact with simulated waste as for the reaction of these gases in the gas phase alone. The primary product of the reaction of nitrous oxide with hydrogen in contact with wet or dried simulated waste is nitrogen, followed by oxygen and other oxides of nitrogen. The production of nitrogen and oxygen was increased considerably with irradiation compared to the experiments performed under thermal conditions alone. The decomposition of hydrogen and nitrous oxide was temperature dependent especially within the irradiated sample in contact with wet simulated waste. An increase in the production of nitrogen with increasing temperature follows the consumption of nitrous oxide for these reactions.

For the reactions of nitrous oxide with hydrogen in contact with wet or dried simulated waste, the mass balance for gas phase nitrogen was not good. The gain of nitrogen is more than can be accounted for by the loss of nitrous oxide alone, most likely due the production of nitrogen from the solid phase sources of nitrogen, nitrite, and nitrate. These solid phase reactants have been shown to produce nitrogen under similar temperature and irradiation conditions in simulated wastes (Bryan and Pederson 1994; Bryan et al. 1992). In contrast to the work reported for the gas phase reactions of nitrous oxide and hydrogen (Bryan and Pederson 1995), when these gases are in contact with simulated waste, no measurable amount of ammonia is produced.

Ammonia was the principal product of the thermal and combined thermal and radiolytic reactions of nitrogen and hydrogen. Radiolytic ammonia yields showed a strong inverse relation with radiation dose. For low radiation doses, $G(NH_3)$ was nearly 1 molecule/100 eV, in good agreement with literature values. However, this yield decreased to approximately 0.01 molecules/100 eV for doses greater than 10 Mrad. From literature results, the value of $G(-NH_3)$ is known to be as much as a factor of ten greater than $G(NH_3)$, depending on temperature and gas partial pressures. As the concentration of NH_3 increased in the gas mixture, so did the relative importance of ammonia decomposition to nitrogen.

The lack of significant quantities of ammonia in either the wet or dried SY1-SIM-92A systems is counter to our observations when only the gas phase nitrogen and hydrogen were present. There is little doubt that this product should form under nearly identical conditions except in the presence of SY1-SIM-92A simulated waste. The absence of ammonia in the systems with waste present is most likely attributed to the reaction of the oxidants nitrite and nitrate with ammonia forming nitrogen, nitrous oxide, and other oxides of nitrogen, which effectively removes ammonia as it is being formed.

The decomposition of ammonia was apparent for the reaction systems containing wet and dry SY1-SIM-92 waste simulant, in both thermal-only and thermal and radiolytic conditions, over the temperature range 60 to 150°C. The reaction of ammonia under thermal-only conditions and under radiolytic and thermal conditions shows a definite trend with increasing temperature. Although there is a definite temperature dependence, the decomposition is more prominently facilitated in the radiolytic experiments. Nitrogen and hydrogen are the principal products of the radiolytic decomposition of ammonia in contact with the wet or dried simulated waste. Hydrogen is produced in a greater fraction in the wet system than in the dried system, most likely due to its co-production by radiolysis of water. Radiolysis of ammonia in the gas phase, coupled with thermal decomposition, may be an important means by which the ultimate concentration of ammonia is limited in Hanford Site wastes.

5.0 References

Anderson, A. R. 1968. *Fundamental Processes in Radiation Chemistry*. P. Ausloos, ed. John Wiley and Sons, New York, p. 281.

Arnold, E. A., and R. E. Burk. 1932. "Thermal Decomposition of Ammonia on the Surface of Osmium." *J. Amer. Chem. Soc.*, 54:23-32.

Ashby, E. C., C. Jonah, D. Meisel, L. R. Pederson, and D. M. Strachan. 1992. *Gas Generation and Retention in Tank 241-SY-101: A Summary of Laboratory Studies, Tank Data, and Information Needs.* PNL-8124, Pacific Northwest Laboratory, Richland, Washington.

Ashby, E. C., F. Doctorovich, C. L. Liotta, H. M. Neumann, E. K. Barefield, A. Konda, K. Zhang, J. Hurley, and D. D. Siemer. 1993. "Concerning the Formation of Hydrogen in Nuclear Waste. Quantitative Generation via a Cannizzaro Intermediate." *J. Am. Chem. Soc.*, 115:1171-1173.

Ashby, E. C., E. K. Barefield, C. L. Liotta, H. M. Neumann, F. Doctorovich, A. Konda, K. Zhang, J. Hurley, D. Boatwright, D. A. Annis, G. Pansino, M. Dawson, and M. Juliao. 1994a. "Mechanistic Studies Related to the Thermal Chemistry of Simulated Nuclear Wastes that Mimic the Contents of a Hanford Site Double-Shell Tank." *Am. Chem. Soc. Symp. Ser.*, 554:249-284.

Ashby, E. C., D. A. Annis, E. K. Barefield, D. Boatwright, F. Doctorovich, C. L. Liotta, H. M. Neumann, A. Konda, C. F. Yao, K. Zhang, and N. G. McDuffie. 1994b. *Synthetic Waste Chemical Mechanism Studies*. WHC-EP-0823, Westinghouse Hanford Company, Richland, Washington.

Babad, H., G. D. Johnson, J. A. Lechelt, D. A. Reynolds, L. R. Pederson, D. M. Strachan, D. Meisel, C. D. Jonah, and E. C. Ashby. 1991. *Evaluation of the Generation and Release of Flammable Gases in Tank 241-SY-101*. WHC-EP-0517, Westinghouse Hanford Company, Richland, Washington.

Babad, H., G. D. Johnson, D. A. Reynolds, and D. M. Strachan. 1992. *"Understanding of Cyclic Venting Phenomena in Hanford Site High-Level Waste Tanks: The Evaluation of Tank 241-SY-101."* WHC-SA-1364-FP, Westinghouse Hanford Company, Richland, Washington.

Baer, D. R., and L. S. Dake. 1986. *Oxidation of Metals and Associated Mass Transport*. M. A. Dayananda, S. J. Rothman, and W. E. King, eds. Metallurgical Society of AIME, New York, p. 185.

Bottomley, F., and R. C. Burns. 1979. *Treatise on Nitrogen Fixation*. Wiley Interscience, New York, p. 50.

Bou-Hamra, W. S. 1988. *Formation of Ammonium Nitrate Aerosols by Gas-Phase Reaction of Ammonia and Nitrogen Dioxide*. Ph.D. Dissertation, Oklahoma State University, Stillwater, Oklahoma.

Briant, C. L., and R. A. Mulford. 1982. "Surface Segregation in Austenitic Stainless Steel." *Met. Trans. A.*, 13A:745-752.

Brown, L.L. 1966 "Isotope Effects in the Alkaline Reduction of NO_3^-, NO_2^-, and NH_2OH by Fe(II); Chemistry Division Annual Progress Report", ORNL-3994, Oak Ridge National Laboratory, Oak Ridge, Tennessee, p. 28.

Bryan, S. A., L. R. Pederson, J. L. Ryan, R. D. Scheele, and J. M. Tingey. 1992. *Slurry Growth, Gas Retention, and Flammable Gas Generation by Hanford Radioactive Waste Tanks: Synthetic Waste Studies*. PNL-8169, Pacific Northwest Laboratory, Richland, Washington.

Bryan, S. A., L. R. Pederson, and R. D. Scheele. 1992. "Crust Growth and Gas Retention in Synthetic Hanford Wastes." *Proceedings of the Waste Management '92 Conference,* 1:829-834. American Nuclear Society, Las Vegas, Nevada.

Bryan, S. A., and L. R. Pederson. 1992. In *Minutes of the Tank Waste Science Panel Meeting March 25-27, 1992.* W. W. Schulz and D. M. Strachan, eds. PNL-8278, Pacific Northwest Laboratory, Richland, Washington.

Bryan, S. A., L. R. Pederson, R. D. Scheele, and S. R. Adami. 1993. In *Proceedings of the 4th Annual International Conference on High Level Radioactive Waste Management,* 2:1348. American Nuclear Society, Las Vegas, Nevada.

Bryan, S. A., and L. R. Pederson. 1994. *Composition, Preparation, and Gas Generation Results from Simulated Wastes of Tank 241-SY-101*. PNL-10075, Pacific Northwest Laboratory, Richland, Washington.

Bryan, S. A., and L. R. Pederson. 1995. *Thermal and Combined Thermal and Radiolytic Reactions Involving Nitrous Oxide, Hydrogen, and Nitrogen in the Gas Phase: Comparison of Gas Generation Rates in Supernate and Solid Fractions of Tank 241-SY-101 Simulated Wastes*. PNL-10490, Pacific Northwest Laboratory, Richland, Washington.

Cotton, F. A., and G. Wilkinson. 1980. *Advanced Inorganic Chemistry, 4th Edition*, p. 418.

CRC Handbook of Radiation Chemistry. 1986. Chemical Rubber Company, Cleveland, Ohio, p. 607.

Cunningham, J. 1963. "Radiation Chemistry of Ionic Solids. III. Chemical Studies on the Formation and Annealing of Radicals in Irradiated Nitrates." *J. Phys. Chem.*, 67:1772-1778.

Delegard, C. 1980. *Laboratory Studies of Complexed Waste Slurry Volume Growth in Tank 241-SY-101*. RHO-LD-124, Rockwell International, Richland, Washington.

Dell, R. M., F. S. Stone, and P. F. Tiley. 1953. "The Decomposition of Nitrous Oxide on Cuprous Oxide and Other Oxide Catalysts." *Trans. Faraday Soc.*, 49:201-209.

Doremus, R. H. 1973. *Glass Science*. John Wiley and Sons, New York, p. 102.

Engell, H. J., and K. Hauffe. 1953. "Der Einfluß der Elektronenfehlordnung Oxydischer Katalysatoren auf die Zerfallsgeschwindigkeit des Stickoxyduls." *Z. Elektrochem.*, 57:776-778.

Garner, W. E., T. J. Gray, and F. S. Stone. 1950. "Reactions on the Surface of Copper Oxide." *Discussions Faraday Soc.*, 8:246-250.

Gauglitz, P. A., R. R. Shah, and R. L. Davis. 1994a. *Gas Distribution Effects on Waste Properties: Viscosities of Bubbly Slurries*. PNL-10112, Pacific Northwest Laboratory, Richland, Washington.

Gauglitz, P. A., L. A. Mahoney, D. P. Mendoza, and M. C. Miller. 1994b. *Mechanisms of Gas Bubble Retention*. PNL-10120, Pacific Northwest Laboratory, Richland, Washington.

Harteck, P., and S. Dondes. 1956. "Nitrous Oxide Dosimeter for High Levels of Betas, Gammas, and Thermal Neutrons." *Nucleonics*, 14(3):66-72.

Hauffe, K., R. Glang, and H. J. Engel. 1950. "The Effect of the Electron Disorder Structure of Oxide Catalysts on the Decomposition of Nitrous Oxide." *Z. Physik. Chem.*, 201:223.

Hearne, J. A., and R. W. Hummel. 1961. "Nitrous Oxide as a Dosimeter for Ionizing Radiations." *Radiation Res.*, 15:254-257.

Herting, D. L., D. B. Bechtold, B. A. Crawford, T. L. Welsh, and L. Jensen. 1992a. *Laboratory Characterization of Samples Taken in May 1991 from Hanford Tank 241-SY-101*. WHC-SE-WM-DTR-024, Westinghouse Hanford Company, Richland, Washington.

Herting, D. L., D. B. Bechtold, B. E. Hey, B. D. Keele, L. Jensen, and T. L. Welsh. 1992b. *Laboratory Characterization of Samples Taken in December 1991 (Window E) from Hanford Waste Tank 241-SY-101*. WHC-SD-WM-DTR-026 Rev. 0, Westinghouse Hanford Company, Richland, Washington.

Hertzberg, M., and I. A. Zlochower. 1994. In *Proceedings of the 25th International Symposium on Combustion*. The Combustion Institute, Pittsburgh, Pennsylvania, p. 254.

Hibben, J. H. 1928. "The Low Pressure Decomposition of Nitric and Nitrous Oxides." *J. Amer. Chem. Soc.*, 50:940-950.

Hinshelwood, C. N., and R. T. Burke. 1925. "The Thermal Decomposition of Ammonia on Various Surfaces." *J. Chem. Soc.*, 127:1105-1117.

Hinshelwood, C. N., and C. R. Pritchard. 1925a. "The Catalytic Decomposition of Nitrous Oxide on the Surface of Gold: A Comparison with the Homogeneous Reaction." *Proc. Royal Soc. (London)*, A108:211-215.

Hinshelwood, C. N., and C. R. Pritchard. 1925b. "A Comparison Between the Homogeneous Thermal Decomposition of Nitrous Oxide and Its Heterogeneous Catalytic Decomposition on the Surface of Platinum." *J. Chem. Soc.*, 127:327-336.

Homann, K. H., and A. Haas. 1972. *Comprehensive Chemical Kinetics, Vol. 4: Decomposition of Inorganic and Organometallic Compounds,* eds. C. H. Bamford and C. F. H. Tipper, p. 1.

Hutchinson, W. H., and C. N. Hinshelwood. 1926. "The Interaction of Hydrogen and Nitrous Oxide on the Surface of Gold." *J. Chem. Soc.*, 129:1556-1559.

Jacobs, T. A. 1963. "Further Shock-Tube Studies by Infrared Emission of the Decomposition of Ammonia." *J. Phys. Chem.*, 67:665-667.

Johnson, G. R. A. 1973. *Radiation Chemistry of Nitrous Oxide Gas. Primary Processes, Elementary Reactions, and Yields*. NSRDS-NBS 45, U.S. Department of Commerce-National Bureau of Standards, Washington, D.C.

Johnston, H. S. 1951. "Interpretation of the Data on the Thermal Decomposition of Nitrous Oxide." *J. Chem. Phys.*, 19:663-668.

Jones, K. 1975. In *Comprehensive Inorganic Chemistry.* J. C. Bailar, H. J. Emeleus, R. Nyholm, and A. F. Trotman-Dickenson, eds. Pergamon Press, New York, p. 147.

Kaufman, F., N. J. Gerri, and R. E. Bowman. 1956. "Role of Nitric Oxide in the Thermal Decomposition of Nitrous Oxide." *J. Chem. Phys.*, 25:106-115.

Kunsman, C. H. 1928. "The Thermal Decomposition of Ammonia in Tungsten, Molybdenum and Nickel. I." *J. Amer. Chem. Soc.*, 50:2100-2113.

Laidler, K. J. 1965. *Chemical Kinetics*. McGraw-Hill, New York, p. 296.

Lindars, F. J., and C. N. Hinshelwood. 1955a. "The Thermal Decomposition of Nitrous Oxide I. Secondary Catalytic and Surface Effects." *Proc. Royal Soc. Series A,* 231:162-178.

Lindars, F. J., and C. N. Hinshelwood. 1955b. "The Thermal Decomposition of Nitrous Oxide II. Influence of Added Gases and a Theory of the Kinetic Mechanism." *Proc. Royal Soc. Series A,* 231:178-197.

Los Alamos National Laboratory (LANL). 1994. *A Safety Assessment for Proposed Pump Mixing Operations to Mitigate Episodic Gas Releases in Tank 241-SY-101: Hanford Site, Richland, Washington*. LA-UR-92-3196 Rev. 9, Los Alamos National Laboratory, Los Alamos, New Mexico.

Meisel, D., H. Diamond, E. P. Horwitz, C. D. Jonah, M. S. Matheson, M. C. Sauer Jr., and J. C. Sullivan. 1991. *Radiation Chemistry of Synthetic Waste*. ANL-91/40, Argonne National Laboratory, Argonne, Illinois.

Meisel, D., H. Diamond, C. D. Jonah, M. C. Sauer Jr., J. C. Sullivan, F. Barnabas, E. Cerny, and Y. D. Cheng. 1992. "Radiolytic and Radiolytically Induced Generation of Gases in Simulated Mixed Waste Solutions." In *Proceedings of Waste Management '92*, 1:859. American Nuclear Society and International Atomic Energy Agency.

Meisel, D., C. D. Jonah, S. Kapoor, M. S. Matheson, and M. C. Sauer, Jr. 1993. *Radiolytic and Radiolytically Induced Generation of Gases From Synthetic Wastes*. ANL-93/43, Argonne National Laboratory, Argonne, Illinois.

Melia, T. P. 1965. "Decomposition of Nitric Oxide at Elevated Pressures." *J. Inorg. Nucl. Chem.*, 27:95-98.

Melville, H. W. 1934. "The Kinetics of the Reaction between Hydrogen and Nitrous Oxide. Part II." *Proc. Roy. Soc. A,* 146:737-775.

Michel, K. W., and H. G. Wagner. 1965. *Tenth International Symp. on Combustion.* The Combustion Institute, Pittsburgh, Pennsylvania, p. 353.

Muhammad, D., and A. G. Maddock. 1978. "Radiolysis of the Alkali Nitrates" *J. Chem. Soc., Faraday Trans.* 1(74):919-932.

Norton, J. D., and L. R. Pederson. 1994. *Ammonia in Simulated Hanford Double-Shell Tank Wastes: Solubility and Effects on Surface Tension*. PNL-10173, Pacific Northwest Laboratory, Richland, Washington.

Norton, J. D., and L. R. Pederson. 1995. *Solubilities of Gases in Simulated Tank 241-SY-101 Wastes*. PNL-10785, Pacific Northwest Laboratory, Richland, Washington.

O"Donnell, J. H., and D. F. Sangster. 1970. *Principles of Radiation Chemistry*. American Elsevier, New York, p. 67.

Orth, R. J., A. J. Schmidt, A. H. Zacher, M. R. Elmore, T. R. Hart, J. C. Poshusta, G. G. Neuenscwander, E. O. Jones, and S. R. Gano. 1993. *Organic Destruction Technology Development Task Annual Report - FY 1993: Hydrothermal Processing of Hanford Tank Waste.* PNL-10108, Pacific Northwest Laboratory, Richland, Washington.

Pasamehmetoglu, K., W. L. Kubic, J. Spore, R. Lin, J. Dearing, and P. Sadasivan. 1994. *101-SY-Modeling Issues*. Los Alamos National Laboratory, Los Alamos, New Mexico.

Pederson, L. R., and S. A. Bryan. 1994. *Assessment of the Potential for Ammonium Nitrate Formation and Reaction in Tank 241-SY-101*. PNL-10067, Pacific Northwest Laboratory, Richland, Washington.

Pourbaix, M. 1974. *Atlas of Electrochemical Equilibria in Aqueous Solutions*. National Association of Corrosion Engineers, Houston, p. 316.

Preston, K. F., and R. J. Cvetanovic. 1972. *Comprehensive Chemical Kinetics, Vol. 4: Decomposition of Inorganic and Organometallic Compounds*, p. 47.

Reynolds, D. A., D. D. Siemer, D. M. Strachan, and R. W. Wallace. 1991. *A Survey of Available Information on Gas Generation in Tank 241-SY-101*. PNL-7520, Pacific Northwest Laboratory, Richland, Washington.

Samsonov, G. V. 1973. *The Oxide Handbook*. IFI-Plenum, New York, p. 210.

Sax, N. I. 1979. *Dangerous Properties of Industrial Materials, 5th Edition*. Van Nostrand Reinhold Company, New York, p. 325.

Schmidt, A. J., E. O. Jones, R. J. Orth, M. E. Elmore, D. C. Meng, G. G. Neuenscwander, and T. R. Hart. 1993. *Preliminary Conceptual Design for the Destruction of Organic/Ferrocyanide Constituents in the Hanford Tank Waste with Low-Temperature Hydrothermal Processing*. PNL-SA-23181, Pacific Northwest Laboratory, Richland, Washington.

Schmidt, A. J., M. E. Elmore, R. J. Orth, R. O. Jones, A. J. Zacher, T. R. Hart, G. G. Neuenscwander, and J. C. Poshusta. 1994. "Organic Destruction to Enhance the Separation of Strontium in Radioactive Wastes." *Metals and Materials Waste Recovery and Remediation*, K. C. Liddell, R. G. Bautista, and R. J. Orth, Eds. Minerals, Metals, and Materials Society, pp. 151-162.

Schwab, G. M., R. Stager, and H. H. von Baumbach. 1933. "Die Stickoxydul Spaltenoe Wirkung von Metalloxyden und ihr Gang im Periodischen System." *Z. Physik. Chem.*, B21:65-83.

Simpson, R. E. 1961. "Current Developments in the Use of Nitrous Oxide in the Radiation Dosimetry Associated with the Radiation Effects Reactor." *Health Physics*, 8:143-154.

Sorokin, Y. A., and S. Y. Pshezhetskii. 1964. "Decomposition of Ammonia by γ-Radiation." *Russ. J. Phys. Chem.*, 38(3):434-436.

Spinks, J. T. W., and R. J. Woods. 1990. *An Introduction to Radiation Chemistry*. John Wiley and Sons, New York, p. 210.

Strachan, D. M., and W. W. Schulz. 1993. *Minutes of the Tank Waste Science Panel Meeting January 12-13, 1993*. PNL-8845, Pacific Northwest Laboratory, Richland, Washington.

Thomas, J. M., and W. J. Thomas. 1969. *Introduction to the Principles of Heterogeneous Catalysis*. Academic Press, New York, p. 408.

Wagner, C., and K. Hauffe. 1938. "The Stationary State of Catalysts in Homogeneous Reactions." *Z. Elektrochem.*, 44:172-178.

Distribution

No. of Copies

Offsite

2 DOE/Office of Scientific and Technical Information

E. K. Barefield
225 North Avenue
Boggs Chemistry Building
Georgia Institute of Technology
Atlanta, GA 30332

B. S. Hudson
Lawrence Livermore National Laboratory, L-221
P.O. Box 808
Livermore, CA 94550

L. Kovach
NUCON
P.O. Box 29151
Columbus, OH 43229

3 Los Alamos National Laboratory
P.O. Box 1664
Los Alamos, NM 87545
Attn: S. Agnew
W. L. Kubic
K. Pasamehmetoglu

D. Meisel
Argonne National Laboratory
9700 South Cass Avenue
Argonne, IL 60439

D. Strachan
Argonne National Laboratory
9700 So. Cass Ave.
Argonne, IL 60439-4837

No. of Copies

W. W. Schulz
727 Sweetleaf Drive
Wilmington, DE 19808

Onsite

2 DOE Richland Operations Office

C. A. Groendyke	S7-54
G. W. Rosenwald	S7-54

3 Other

M. H. Campbell (MacTec)	S7-73
L. M. Stock	S7-14
J. R. White (LANL)	H5-09

21 Westinghouse Hanford Company

H. Babad	S7-30
G. S. Barney	T5-12
W. B. Barton	R2-11
R. J. Cash	S7-15
K. A. Gasper	G3-21
D. L. Herting	T6-09
J. D. Hopkins	R2-11
J. R. Jewett	T6-09
G. D. Johnson (3)	S7-15
N. W. Kirch	R2-11
J. W. Lentsch	S7-15
E. J. Lipke	S7-14
D. M. Ogden	H0-34
J. C. Person	T6-09
D. A. Reynolds	R2-11
G. R. Sawtelle	A3-37
E. R. Siciliano	H0-31
R. J. Van Vleet	A3-34
N. E. Wilkins	R2-11

No. of Copies		
67	Pacific Northwest National Laboratory	
	Z. I. Antoniak	K7-15
	S. Q. Bennett	K7-90
	P. R. Bredt	P7-25
	M. E. Brewster	K7-15
	J. W. Brothers (15)	K9-20
	S. A. Bryan (20)	P7-25
	L. L. Burger	P7-25
	D. M. Camaioni	K2-44
	J. A. Campbell	P8-08
	C. D. Carlson	P7-25
	P. A. Gauglitz	P7-41
	S. C. Goheen	P8-08
	R. T. Hallen	P8-38
	J. G. Hill	K9-62
	J. D. Hudson	K7-15
	L. G. Morgan	K9-62
	L. R. Pederson (10)	K2-44
	W. D. Samuels	K2-44
	R. D. Scheele	P7-25
	C. W. Stewart	K7-15
	J. M. Tingey	P7-25
	T. W. Wood	K7-94
	Information Release (3)	K1-06